Seasonal influences on surface ozone variability in continental South Africa and implications for air quality

Tracey Leah Laban[1], Pieter Gideon van Zyl[1]*, Johan Paul Beukes[1], Ville Vakkari[2], Kerneels Jaars[1], Nadine Borduas-Dedekind[3], Miroslav Josipovic[1], Anne Mee Thompson[4], Markku Kulmala[5], and Lauri Laakso[2]

1 Unit for Environmental Sciences and Management, North-West University, Potchefstroom, South Africa
2 Finnish Meteorological Institute, Helsinki, Finland
3 Department of Environmental Systems Science, ETH Zürich, Zürich, Switzerland
4 NASA/Goddard Space Flight Center, Greenbelt, Maryland, USA
5 Department of Physics, University of Helsinki, Finland

*Correspondence to: P.G. van Zyl (pieter.vanzyl@nwu.ac.za)

Abstract

Although elevated surface ozone (O_3) concentrations are observed in many areas within southern Africa, few studies have investigated the regional atmospheric chemistry and dominant atmospheric processes driving surface O_3 formation in this region. Therefore, an assessment of comprehensive continuous surface O_3 measurements performed at four sites in continental South Africa was conducted. The regional O_3 problem was evident, with O_3 concentrations regularly exceeding the South African air quality standard limit, while O_3 levels were higher compared to other background sites in the Southern Hemisphere. The temporal O_3 patterns observed at the four sites resembled typical trends for O_3 in continental South Africa, with O_3 concentrations peaking in late winter and early spring. Increased O_3 concentrations in winter were indicative of increased emissions of O_3 precursors from household combustion and other low-level sources, while a spring maximum observed at all the sites was attributed to increased regional biomass burning. Source area maps of O_3 and CO indicated significantly higher O_3 and CO concentrations associated with air masses passing over a region with increased seasonal open biomass burning, which indicated CO associated with open biomass burning as a major source of O_3 in continental South Africa. A strong correlation between O_3 on CO was observed, while O_3 levels remained relatively constant or decreased with increasing NO_x, which supports a VOC-limited regime. The

instantaneous production rate of O_3 calculated at Welgegund indicated that ~40% of O_3 production occurred in the VOC-limited regime. The relationship between O_3 and precursor species suggests that continental South Africa can be considered VOC-limited, which can be attributed to high anthropogenic emissions of NO_x in the interior of South Africa. The study indicated that the most effective emission control strategy to reduce O_3 levels in continental South Africa should be CO and VOC reduction, mainly associated with household combustion and regional open biomass burning.

Keywords: ozone (O_3) production, NO_x-limited, VOC-limited, biomass burning, regional O_3, air quality

1. Introduction

High surface O_3 concentrations are a serious environmental concern due to their detrimental impacts on human health, crops and vegetation (National Research NRC, 1991). Photochemical smog, comprising O_3 as a constituent together with other atmospheric oxidants, is a major air quality concern on urban and regional scales. Tropospheric O_3 is also a greenhouse gas that directly contributes to global warming (IPCC, 2013).

Tropospheric O_3 concentrations are regulated by three processes, i.e. chemical production/destruction, atmospheric transport, and losses to surface through dry deposition (Monks et al., 2015). The photolysis of nitrogen dioxide (NO_2) in the presence of sunlight is the only known way of producing O_3 in the troposphere (Logan, 1985). O_3 can recombine with nitric oxide (NO) to regenerate NO_2, which will again undergo photolysis to regenerate O_3 and NO. This continuous process is known as the NO_x-dependent photostationary state (PSS) and results in no net production or consumption of ozone (null cycle). However, net production of O_3 in the troposphere occurs outside the PSS when peroxy radicals (HO_2 and RO_2) alter the PSS by oxidising NO to produce 'new' NO_2 (Cazorla and Brune, 2010), resulting in net O_3 production. The main source of these peroxy radicals in the atmosphere is the reaction of the hydroxyl radical ($OH^{\bullet}$) with volatile organic compounds (VOCs) or carbon monoxide (CO) (Cazorla and Brune, 2010).

O_3 precursor species can be emitted from natural and anthropogenic sources. Fossil fuel combustion is considered to be the main source of NO_x in South Africa, which includes coal-fired

power-generation, petrochemical operations, transportation and residential burning (Wells et al., 1996; Held et al., 1996). Satellite observations indicate a well-known NO_2 hotspot over the South African Highveld (Lourens et al., 2012) attributed to industrial activity in the region. CO is produced from three major sources, i.e. fossil fuel combustion, biomass burning, as well as the oxidation of methane (CH_4) and VOCs (Novelli et al., 1992). Anthropogenic sources of VOCs are largely due to industrial and vehicular emissions (Jaars et al., 2014), while biogenic VOCs are also naturally emitted (Jaars et al., 2016). Regional biomass burning, which includes household combustion for space heating and cooking, agricultural waste burning and open biomass burning (wild fires), is a significant source of CO, NO_x and VOCs (Macdonald et al., 2011; Crutzen and Andreae, 1990; Galanter et al., 2000; Simpson et al., 2011) in southern Africa. In addition, stratospheric intrusions of O_3-rich air to the free troposphere can also lead to elevated tropospheric O_3 concentrations (Diab et al., 1996; Diab et al, 2004). O_3 production from natural precursor sources, the long-range transport of O_3 and the injections from stratospheric O_3 contribute to background O_3 levels, which is beyond the control of regulators (Lin et al., 2012).

Since O_3 concentrations are regulated in South Africa, O_3 monitoring is carried out across South Africa through a network of air quality monitoring stations established mainly by provincial governments, local municipalities and industries (http://www.saaqis.org.za). High O_3 concentrations are observed in many areas within the interior of South Africa, which exceed the South African standard O_3 limit, i.e. an eight-hour moving average of 61 ppb (e.g. Laakso et al., 2013). These exceedances can be attributed to high anthropogenic emissions of NO_x and VOCs in dense urban and industrial areas (Jaars et al., 2014), regional biomass burning (Lourens et al., 2011), and O_3 conducive meteorological conditions (e.g. sunlight). Since O_3 is a secondary pollutant, high levels of O_3 can also be found in rural areas downwind of city centres and industrial areas. In order for South Africa to develop an effective management plan to reduce O_3 concentrations by controlling NO_x and VOC emissions, it is important to determine whether a region is NO_x- or VOC-limited. However, O_3 production has a complex and non-linear dependence on precursor emissions (e.g. National Research NRC, 1991), which makes its atmospheric levels difficult to control (Holloway and Wayne, 2010). Under VOC-limited conditions, O_3 concentrations increase with increasing VOCs, while a region is considered NO_x-limited when O_3 production increases with increasing NO_x concentrations. Results from a photochemical box model study in South Africa, for instance, revealed that the Johannesburg-Pretoria megacity is within a VOC-limited regime (Lourens et al., 2016). VOC reductions would, therefore, be most effective in reducing O_3, while NO_x controls without VOC controls may lead to O_3 increases. In general, it is

considered that O_3 formations in regions close to anthropogenic sources are VOC-limited, while rural areas distant from source regions are NO_x-limited (Sillman, 1999).

Previous assessments of tropospheric O_3 over continental South Africa have focused on surface O_3 (Venter et al., 2012; Laakso et al., 2012; Lourens et al., 2011; Josipovic et al., 2010; Zunckel et al., 2004), as well as free tropospheric O_3 based on soundings and aircraft observations (Diab et al., 1996; Thompson, 1996; Swap et al., 2003; Diab et al., 2004). Two major field campaigns (SAFARI-92 and SAFARI 2000) were conducted to improve the understanding of the effects of regional biomass burning emissions on O_3 over southern Africa. These studies indicated a late winter-early spring (August and September) maximum over the region that was mainly attributed to increased regional open biomass burning during this period, while Lourens et al. (2011) also attributed higher O_3 concentrations in spring in the Mpumalanga Highveld to increased regional open biomass burning. A more recent study demonstrated that NO_x strongly affects O_3 levels in the Highveld, especially in winter and spring (Balashov et al., 2014). A regional photochemical modelling study (Zunckel et al., 2006) has attempted to explain surface O_3 variability, which found no dominant source/s on elevated O_3 levels.

The aim of the current study is to provide an up-to-date assessment of the seasonal and diurnal variations in surface O_3 concentrations over continental South Africa, as well as to identify local and regional sources of precursors contributing to surface O_3. Another objective is to use available ambient data to qualitatively assess whether O_3 formation is NO_x- or VOC-limited in different environments. An understanding of the key precursors that control surface O_3 production is critical for the development of an effective O_3 control strategy.

2. Methodology

2.1 Study area and measurement stations

Continuous in-situ O_3 measurements obtained from four research stations in the north-eastern interior of South Africa, indicated in Fig. 1, which include Botsalano (25.54^o S, 25.75^o E, 1420 m a.s.l.), Marikana (25.70^o S, 27.48^o E, 1170 m a.s.l.), Welgegund (26.57 ^{o} S, 26.94^o E, 1480 m a.s.l.) and Elandsfontein (26.25^o S, 29.42^o E, 1750 m a.s.l.), were analysed. This region is the largest industrial (indicated by major point sources in Fig. 1) area in South Africa, with substantial gaseous and particulate emissions from numerous industries, domestic fuel burning and vehicles

(Lourens et al., 2012; Lourens et al., 2011), while the Johannesburg-Pretoria megacity is also located in this area (Fig. 1). A combination of meteorology and anthropogenic activities has amplified the pollution levels within the region. The seasons in South Africa correspond to typical austral seasons, i.e. winter from June to August, spring from September to November, summer from December to February and autumn from March to May. The climate is semi-arid with an annual average precipitation of approximately 400 to 500 mm (Klopper et al., 2006; Dyson et al., 2015), although there is considerable inter-annual variability associated with El Niño Southern Oscillation (ENSO) phenomena. Precipitation in the north-eastern interior occurs mostly during the austral summer, from October to March, whereas the region is characterised by a distinct cold and dry season from May to September, i.e. late autumn to mid-spring, during which almost no precipitation occurs. During this period, the formation of several inversion layers is present in the region, which limits the vertical dilution of air pollution, while more pronounced anticyclonic recirculation of air masses also occurs. This synoptic-scale meteorological environment leads to an accumulation of pollutants in the lower troposphere in this region, which can be transported for several days (Tyson and Preston-Whyte, 2000; Garstang et al., 1996). The SAFARI-92 and SAFARI 2000 campaigns indicated that locations in southern Africa, thousands of kilometres apart, are linked through regional anticyclonic circulation (Swap et al., 2003).

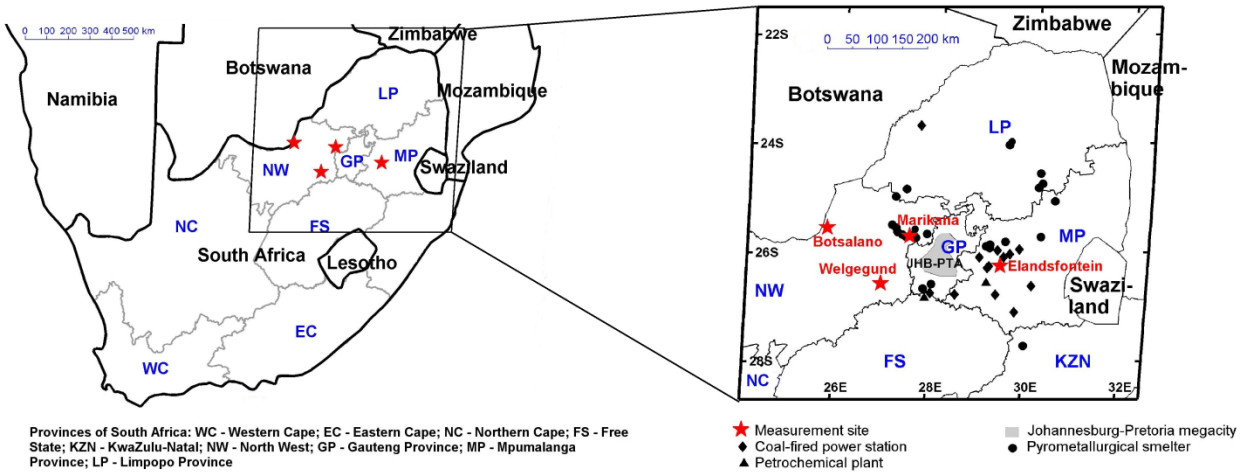

Fig. 1. Location of the four measurement sites in South Africa

2.1.1 Botsalano

The Botsalano measurement site is situated in a game reserve in the North West Province of South Africa, which is considered to be representative of regional background air. The surrounding vegetation is typical of a savannah biome, consisting of grasslands with scattered shrubs and trees (Laakso et al., 2008). The area is quite sparsely populated and has no local anthropogenic pollution sources (Laakso et al., 2008; Vakkari et al., 2013). The western Bushveld Igneous Complex, where numerous platinum, base metal, vanadium and chromium mining/smelting industries are situated, is the largest regional anthropogenic pollution source, with the Rustenburg area located approximately 150 km to the east. Botsalano is also occasionally impacted by plumes passing over the industrialised Mpumalanga Highveld and the Johannesburg-Pretoria megacity (Laakso et al., 2008; Vakkari et al., 2011). In addition, the site is influenced by seasonal regional savannah wildfires during the dry period (Laakso et al., 2008; Vakkari et al., 2011; Mafusire et al., 2016). Measurements were conducted from 20 July 2006 until 5 February 2008 (Laakso et al., 2008; Vakkari et al., 2011; Vakkari et al., 2013).

2.1.2 Marikana

The Marikana measurement site is located within the western Bushveld Igneous Complex, which is a densely populated and highly industrialised region, where mining and smelting are the predominant industrial activities. Marikana is a small mining town located approximately 30 km east of Rustenburg and approximately 100 km northwest of Johannesburg. The measurement site is located in the midst of a residential area, comprising low-cost housing settlements and municipal buildings (Hirsikko et al., 2012; Venter et al., 2012). Anthropogenic emissions from household combustion, traffic and industry in the wider region have a strong influence on the measurement site (Venter et al., 2012). Data was collected from 8 February 2008 to 16 May 2010 and has been previously used in other studies (Venter et al., 2012; Vakkari et al., 2013; Petäjä et al., 2013; Hirsikko et al., 2012; Hirsikko et al., 2013).

2.1.3 Welgegund

This measurement site is approximately 100 km west of Johannesburg and is located on a commercial arable and pastoral farm. The station is surrounded by grassland savannah (Jaars et al., 2016). The station can be considered a regionally representative background site with few

local anthropogenic sources. Air masses arriving at Welgegund from the west reflect a relatively clean regional background. However, the site is, similar to the Botsalano station, at times impacted by polluted air masses that are advected over major anthropogenic source regions in the interior of South Africa, which include the western Bushveld Igneous Complex, the Johannesburg-Pretoria megacity, the Mpumalanga Highveld and the Vaal Triangle (Tiitta et al., 2014; Jaars et al., 2016; Venter et al., 2017). In addition, Welgegund is also affected by regional savannah and grassland fires that are common in the dry season (Vakkari et al., 2014). The atmospheric measurement station has been operating at Welgegund since 20 May 2010, with data measured up until 31 December 2015 utilised in this study.

2.1.4 Elandsfontein

Elandsfontein is an ambient air quality monitoring station operated by Eskom, the national electricity supply company, primarily for legislative compliance purposes. This station was upgraded and co-managed by researchers during the EUCAARI project (Laakso et al., 2012). The Elandsfontein station is located within the industrialised Mpumalanga Highveld at the top of a hill approximately 200 km east of Johannesburg and 45 km south-southeast of eMalahleni (previously known as Witbank), which is a coal mining area (Laakso et al., 2012). The site is influenced by several emission sources, such as coal mines, coal-fired power-generating stations, a large petrochemical plant and traffic emissions. Metallurgical smelters to the north also frequently impact the site (Laakso et al., 2012). The Elandsfontein dataset covers the period 11 February 2009 until 31 December 2010 during the EUCAARI campaign (Laakso et al., 2012).

2.2 Measurements

A comprehensive dataset of continuous measurements of surface aerosols, trace gases and meteorological parameters has been acquired through these four measurement sites (Laakso et al., 2008; Vakkari et al., 2011; Venter et al., 2012; Laakso et al., 2012; Vakkari et al., 2013; Petäjä et al., 2013). In particular, ozone (O_3, nitric oxide (NO), nitrogen dioxide (NO_2) and carbon monoxide (CO), as well as meteorological parameters, such as temperature (^oC) and relative humidity (%) measurements were used in this study. Note that Botsalano, Marikana and Welgegund measurements were obtained with the same mobile station (first located at Botsalano, then relocated to Marikana and thereafter permanently positioned at Welgegund), while Elandsfontein measurements were conducted with a routine monitoring station. O_3 concentrations

at Welgegund, Botsalano and Marikana research stations were measured using the Environment SA 41M O_3 analyser, while a Monitor Europe ML9810B O_3 analyser was utilised at Elandsfontein. CO concentrations were determined at Welgegund, Botsalano and Marikana with a Horiba APMA-360 analyser, while CO was not measured at Elandsfontein. NO_x ($NO+NO_2$) concentrations were determined with a Teledyne 200AU NO/NO_x analyser at Welgegund, Botsalano and Marikana, whereas a Thermo Electron 42i NOx analyser was used at Elandsfontein. Temperature and relative humidity were measured with a Rotronic MP 101A instrument at all the sites.

Data quality at these four measurement sites was ensured through regular visits to the sites, during which instrument maintenance and calibrations were performed. The data collected from these four stations was subjected to detailed cleaning (e.g. excluding measurements recorded during power interruptions, electronic malfunctions, calibrations and maintenance) and the verification of data quality procedures (e.g. corrections were made to data according to in-situ calibrations and flow-checks). Therefore, the datasets collected at all four measurement sites are considered to represent high quality, high resolution measurements as indicated by other papers (Laakso et al., 2008; Petäjä et al., 2013; Venter et al., 2012; 2011; Laakso et al., 2012; Vakkari et al., 2013). Detailed descriptions of the data post-processing procedures were presented by Laakso et al. (2008) and Venter et al. (2012). The data was available as 15-minute averages and all plots using local time (LT) refer to local South African time, which is UTC+2.

In order to obtain a representative spatial coverage of continental South Africa, O_3 data from an additional 54 ambient monitoring sites was selected. These included O_3 measurements from 18 routine monitoring station measurements (SAAQIS) for the period January 2012 to December 2014 (downloaded from the JOIN web interface https://join.fz-juelich.de (Schultz et al., 2017)) and 36 passive sampling sites located in the north-eastern interior of South Africa where monthly O_3 concentrations were determined for two years from 2006 to 2007 (Josipovic, 2009). Spatial analyses were conducted with a geographic information system mapping tool (ArcGIS software), which used ordinary kriging to interpolate the O_3 concentrations measured at the 58 sites in order to build the spatial distribution. The interpolation method involved making an 80/20% split of the data (80% for model development, 20% for evaluation), where 20% were used to calculate the root squared mean error (RSME = 0.2804331). Optimal model parameters were selected using an iterative process and evaluated on the basis of the best performance statistics obtained (reported in the ArcGIS kriging output), with particular emphasis on minimising the RSME. The

extent of area was 23.00154974 (top), -29.03070026 (bottom), 25.74238974 (left) and 32.85246366 (right).

2.3 Air mass history

Individual hourly four-day back trajectories for air masses arriving at an arrival height of 100 m above ground-level were calculated for the entire measurement period at each monitoring site, using HYSPLIT 4.8 (Hybrid Single-Particle Langrangian Integrated Trajectory model) (Stein et al., 2015; Draxler and Hess, 1998). The model was run with the GDAS meteorological archive produced by the US National Weather Service's National Centre for Environmental Prediction (NCEP) and archived by ARL (Air Resources Laboratory, 2017). Overlay back trajectory maps were generated by superimposing individual back trajectories onto a southern African map divided into 0.5° X 0.5°grid cells. In addition, source maps were compiled by assigning each grid cell with a mean measured O_3 and CO concentration associated with trajectories passing over that cell, similar to previous methods (Vakkari et al., 2011; Vakkari et al., 2013; Tiitta et al., 2014). A minimum of ten trajectories per cell were required for the statistical reliability.

2.4 Modelling instantaneous production rate of O_3

The only speciated VOC dataset available and published in South Africa exists for Welgegund (Jaars et al., 2016; Jaars et al., 2014), which could be used to model instantaneous O_3 production at this site. The concentration of these biogenic and anthropogenic VOCs was obtained from grab samples taken between 11:00 and 13:00 LT over the course of two extensive field campaigns conducted from February 2011 to February 2012 and from December 2013 to February 2015. During this time, six trace gases, 19 biogenic VOCs and 20 anthropogenic VOCs, including 13 aromatic and seven aliphatic compounds were measured. The VOC reactivity was calculated from the respective rate coefficients of each VOC with •OH radicals obtained from chemical kinetic databases such as JPL, NIST and the MCM (e.g. Jaars et al., 2014) to estimate ozone production at 11:00 LT at Welgegund. Specifically, each VOC reactivity was then summed to obtain the total VOC reactivity for each measurement, i.e. VOC reactivity = $\sum k_{1i}[VOC]_i$. The major contributors to VOC reactivity are depicted in Fig. A1 and include, in approximate order of contribution, *o*-xylene, CO, styrene, *p*,*m*-xylene, toluene, ethylbenzene limonene, isoprene, α-pinene, β-pinene and hexane. Of note, key compounds such as methane are not included, which could contribute to VOC reactivity, and therefore this VOC reactivity can only be a lower estimate. However, if a

global ambient concentration of 1.85 ppm and a rate of oxidation by •OH radicals of 6.68×10^{-15} cm^3 $molec^{-1}$ s^{-1} are assumed (Srinivasan et al., 2005), a VOC reactivity of 0.3 s^{-1} would be obtained and would therefore account for a small increase in the VOC reactivity calculated in Fig. A1 and Fig. 10.

A mathematical box-model was applied to model O_3 production as a function of VOC reactivity and NO_2 concentrations. This model involves three steps, i.e. (1) the estimation of HO_x (sum of •OH and HO_2• radicals) production, (2) the estimation of the •OH radical concentration, and (3) the calculation for O_3 production (Murphy et al., 2006; Geddes et al., 2009). The VOC concentrations are the limiting factor in the ability to model O_3 production at Welgegund, since only data for the 11:00 to 13:00 LT grab samples was available (Fig. A1). Therefore, the model approach does not coincide with peak O_3 typically observed around 14:00 to 15:00 LT, and therefore likely represents a lower estimate.

The production rate of HO_x ($P(HO_x)$) depends on the photolysis rate of O_3 (J_{O3}), concentration of O_3 and vapour pressure of water (Jaegle et al., 2001). The photolysis rate proposed for the Southern Hemisphere, i.e. $J_{O3} = 3 \times 10^{-5}$ s^{-1} (Wilson, 2015), was used, from which $P(HO_x)$ was calculated as follows:

$$P(HO_X) = 2J_{O3}k_{O3}[O_3][H_2O]$$

and estimated to be 6.09×10^6 molec cm^{-3} s^{-1} or 0.89 ppbv h^{-1} (calculated for a campaign O_3 average of 41 ppbv and a campaign RH average of 42 % at 11:00 LT each day) at STP. The $P(HO_x)$ at Welgegund is approximately a factor of two lower compared to other reported urban $P(HO_x)$ values (Geddes et al., 2009). The factors and reactions that affect [•OH] include:

- linear dependency between •OH and NO_x due to the reaction $NO + HO_2 \rightarrow$ •OH + NO_2, until •OH begins to react with elevated NO_2 concentrations to form HNO_3 ($OH + NO_2 + M \rightarrow HNO_3 + M$);
- $P(HO_x)$ is affected by solar irradiance, temperature, O_3 concentrations, humidity; and
- partitioning of HO_x between RO_2, HO_2, OH.

[•OH] was calculated at 11:00 LT each day as follows:

$$A = k_{5eff}\left(\frac{VOC\ reactivity}{k_{2eff}[NO]}\right)^2$$

$$B = k_4[NO_2] + \alpha * VOC\ reactivity$$

$$C = P(HO_x)$$

$$[OH] = \frac{-B + \sqrt{B^2 + 24C * A}}{12 * A}$$

The instantaneous production rate of O_3, $P(O_3)$ could then be calculated as a function of NO_2 levels and VOC reactivity. A set of reactions used to derive the equations that describe the dependence of the •OH, peroxy radicals (HO_2•+RO_2•) and $P(O_3)$ on NO_x is given by Murphy et al. (2006), which presents the following equation to calculate $P(O_3)$:

$$P(O_3) = k_{2eff}[HO_2 + RO_2][NO] = 2 * VOC\ Reactivity * [OH]$$

where $k_2$eff is the effective rate constant of NO oxidation by peroxy radicals (chain propagation and -termination reactions in the production of O_3). The values of the rate constants and other parameters used as input parameters to solve the equation above can be found in Murphy et al. (2006) and Geddes et al. (2009).

3. Results and discussion

3.1 Temporal variation of O_3

In Fig. 2, the monthly and diurnal variations for O_3 concentrations measured at the four sites in this study are presented (time series plotted in Fig. A2). Although there is some variability between the sites, monthly O_3 concentrations show a well-defined seasonal variation at all four sites, with maximum concentrations occurring in late winter and spring (August to November), which is expected for the South African interior as indicated above and previously reported (Zunckel et al., 2004; Diab et al., 2004). In Fig., A3 monthly averages of meteorological parameters and total monthly rainfall for Welgegund are presented to indicate typical seasonal meteorological patterns for continental South Africa. These O_3 peaks in continental South Africa generally point to two major contributors of O_3 precursors, i.e. open biomass burning (wild fires) (Vakkari et al., 2014), and increased low-level anthropogenic emissions, e.g. increased household combustion for space heating and cooking (Oltmans et al., 2013; Lourens et al., 2011). In addition to the seasonal patterns of O_3 precursor species, during the dry winter months, synoptic scale recirculation is more predominant and inversion layers are more pronounced, while precipitation is minimal (e.g.

Tyson and Preston-Whyte, 2000). These changes in meteorology result in the build-up of precursor species that reach a maximum in August/September when photochemical activity starts to increase. The diurnal concentration profiles of O_3 at the four locations follow the typical photochemical cycle, i.e. increasing during daytime in response to maximum photochemical production and decreasing during the night-time due to titration with NO. O_3 levels peaked from midday to afternoon, with a maximum at approximately 15:00 (LT, UTC+2). From Fig. 2, it is also evident that night-time titration of O_3 at Marikana is more pronounced as indicated by the largest difference between daytime and night-time O_3 concentrations in comparison to the other sites, especially compared to Elandsfontein where night-time concentrations of O_3 remain relatively high in winter.

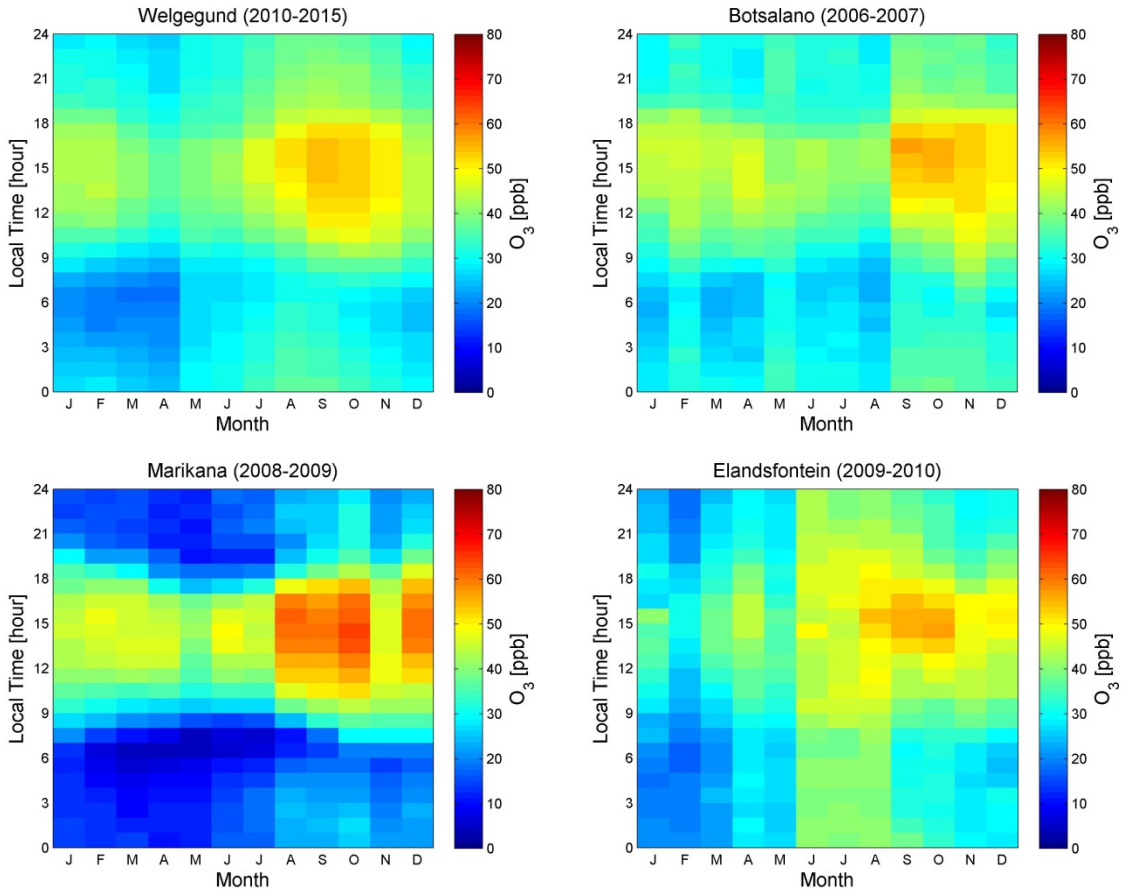

Fig. 2. Seasonal and diurnal variation of median O_3 concentrations at Welgegund, Botsalano, Marikana and Elandsfontein. The O_3 measurement periods varied among sites, which combined spanned a period from July 2006 to December 2015.

3.2 Spatial distribution of O_3 in continental South Africa

Fig. 3 depicts the spatial pattern of mean surface O_3 concentrations over continental South Africa during springtime (S-O-N), when O_3 is usually at a maximum as indicated above. Also presented in Fig. 3, are 96-hour overlay back trajectory maps for the four main study sites over the corresponding springtime periods. The mean O_3 concentration over continental South Africa ranged from 20 ppb to 60 ppb during spring. From Fig. 3, it can be seen that O_3 concentrations at the industrial sites Marikana and Elandsfontein were higher than O_3 levels at Botsalano and Welgegund. As mentioned previously, Elandsfontein is located within the industrialised Mpumalanga Highveld with numerous large point sources of O_3 precursor species. It is also evident from Fig. 3 that rural measurement sites downwind from Elandsfontein, such as Amersfoort, Harrismith and Glückstadt had significantly higher O_3 concentrations, which can be attributed to the formation of O_3 during the transport of precursor species from source regions. Lourens et al. (2011) indicated that higher O_3 concentrations were associated with sites positioned in more rural areas in the Mpumalanga Highveld. Venter et al. (2012) attributed high O_3 concentrations at Marikana, which exceeded South African standard limits on a number of occasions, to the influence of local household combustion for cooking and space heating, as well as to regional air masses with high O_3 precursor concentrations. Higher O_3 concentrations were also measured in the north-western parts of Gauteng, at sites situated within close proximity to the Johannesburg-Pretoria megacity, while the rural Vaalwater site in the north also has significantly higher O_3 levels. From Fig. 3, it is evident that O_3 can be considered a regional problem with O_3 concentrations being relatively high across continental South Africa during spring. Fig. 3 also clearly indicates that the four research sites where surface O_3 was assessed in this study are representative of continental South Africa.

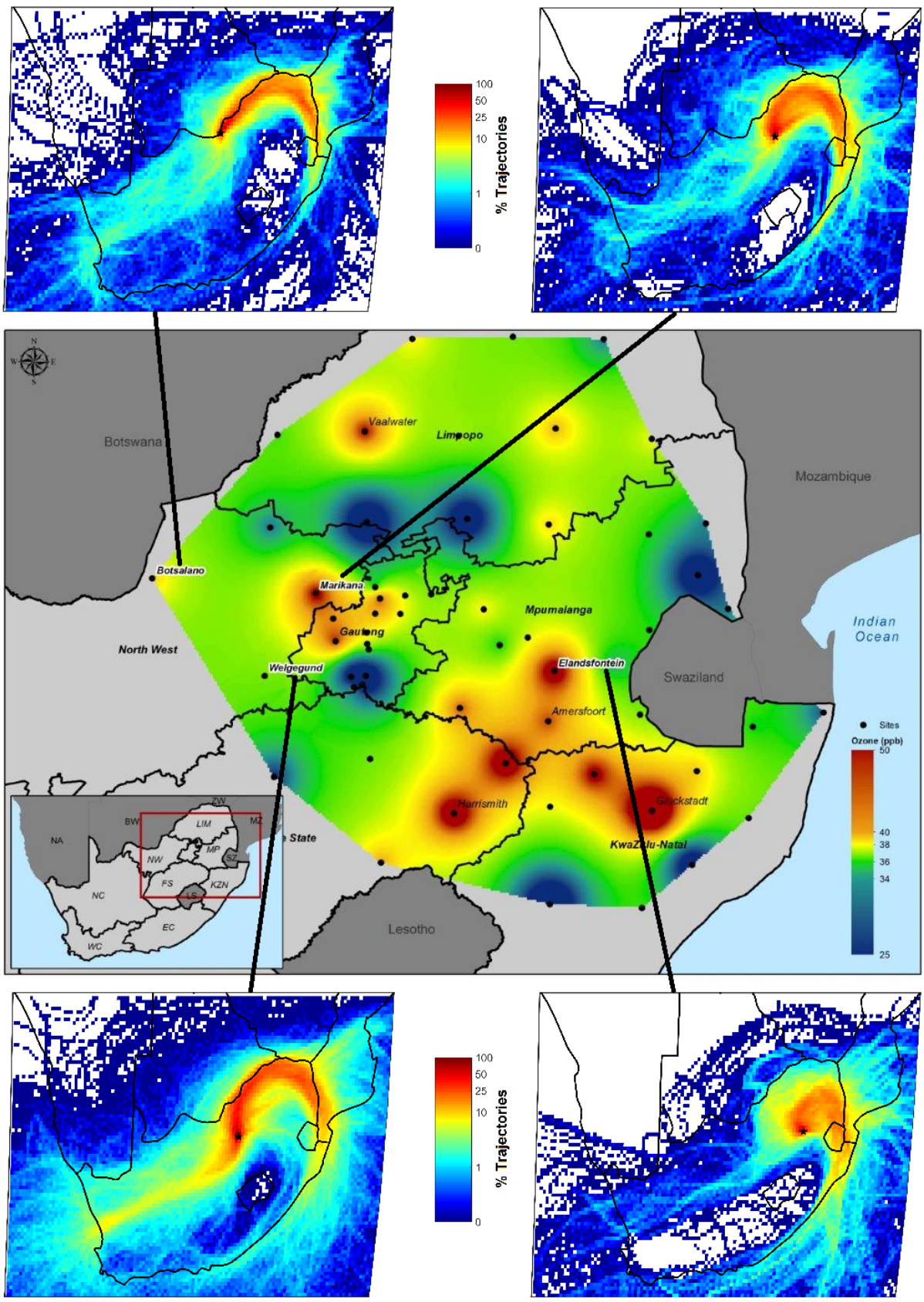
100
50
25
10
1
0
% Trajectories
Botswana
Mozambique
Swaziland
Lesotho
Indian Ocean
Vaalwater
Limpopo
Botsalano
Marikana
Mpumalanga
Gauteng
North West
Welgegund
Elandsfontein
Amersfoort
Harrismith
Glückstadt
KwaZulu-Natal
Free State
Sites
Ozone (ppb)
50
40
38
36
34
25
ZW
BW
LIM
MZ
NA
NW
MP
SZ
FS
KZN
NC
LS
EC
WC

Fig. 2. The main (central) map indicating spatial distribution of mean surface O_3 levels during springtime over the north-eastern interior of southern Africa ranging between 23.00 º S and 29.03 º S, and 25.74 º E and 32.85 º E. The data for all sites was averaged for years when the ENSO cycle was not present (by examining SST anomalies in the Niño 3.4 region). Black dots indicate the sampling sites. The smaller maps (top and bottom) indicate 96-hour overlay back trajectory maps for the four main study sites, over the corresponding springtime periods.

3.3 Comparison with international sites

In an effort to contextualise the O_3 levels measured in this study, the monthly O_3 concentrations measured at Welgegund were compared to monthly O_3 levels measured at monitoring sites in other parts of the world (downloaded from the JOIN web interface https://join.fz-juelich.de (Schultz et al., 2017)) as indicated in Fig. 4. Welgegund was used in the comparison since it had the most extensive data record, while the measurement time period considered was from May 2010 to December 2014. The seasonal O_3 cycles observed at other sites in the Southern Hemisphere are comparable to the seasonal cycle at Welgegund, with slight variations in the time of year when O_3 peaks as indicated in Fig. 4. Cape Grim, Australia; GoAmazon T3 Manancapuru, Brazil; Ushuaia, Argentina; and El Tololo, Chile are regional background GAW (Global Atmosphere Watch) stations with O_3 levels lower than the South African sites. However, the O_3 concentrations at El Tololo, Chile are comparable to Welgegund. Oakdale, Australia and Mutdapliiy, Australia are semi-rural and rural locations, which are influenced by urban and industrial pollution sources, which also had lower O_3 concentrations compared to Welgegund.

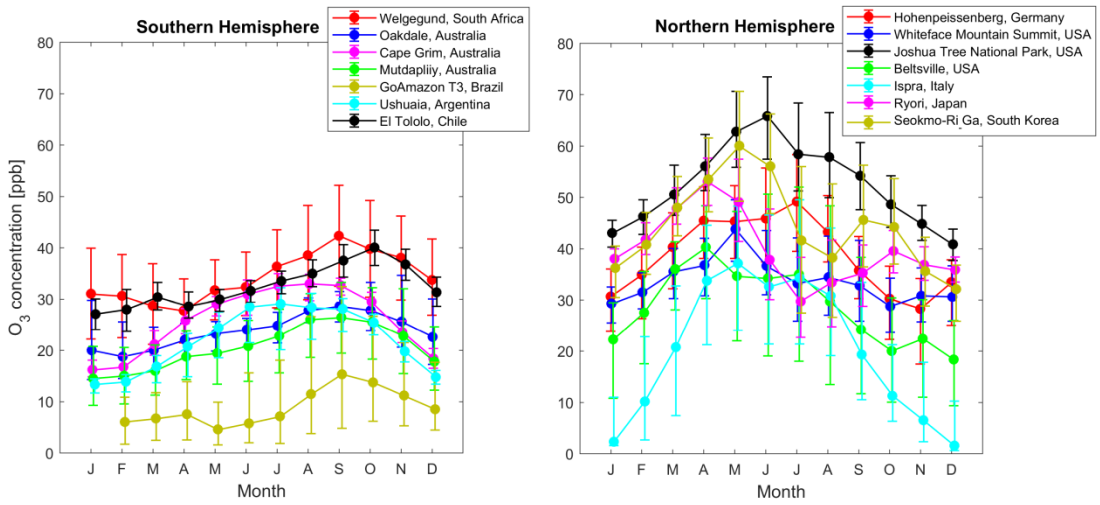

Fig. 4. Seasonal cycle of O_3 at rural sites in other parts of the world. The dots indicate monthly median (50th percentile) and the upper and lower limits the 25th and 75th percentile, respectively for monthly O_3 concentrations. The data is averaged from May 2010 to December 2014, except in a few instances where 2014 data was not available.

The Northern Hemispheric O_3 peak over mid-latitude regions is similar to seasonal patterns in the Southern Hemisphere where a springtime O_3 maximum is observed (i.e. Whiteface Mountain Summit, Beltsville, Ispra, Ryori and Seokmo-Ri Ga). However, there are other sites in the Northern Hemisphere where a summer maximum is more evident (Vingarzan, 2004), i.e. Joshua Tree and Hohenpeissenberg. The discernible difference between the hemispheres is that the spring maximum in the Southern Hemisphere refers to maximum O_3 concentrations in late winter and early spring, while in the Northern Hemisphere, it refers to a late spring and early summer O_3 maximum (Cooper et al., 2014). The spring maximum in the Northern Hemisphere is associated with stratospheric intrusions (Zhang et al., 2014; Parrish et al., 2013), while the summer maximum is associated with photochemical O_3 production from anthropogenic emissions of O_3 precursors being at its highest (Logan, 1985; Chevalier et al., 2007). Maximum O_3 concentrations at background sites in the United States and Europe are similar to values at Welgegund in spring with the exception of Joshua Tree National Park in the United States, which had significantly higher O_3 levels. This is most likely due its high elevation and deep boundary layer (~4 km asl) during spring and summer allowing free tropospheric O_3 to be more effectively mixed down to the surface (Cooper et al., 2014). Maximum O_3 levels at the two sites in East Asia (Ryori and Seokmo-Ri Ga) were also generally higher than at Welgegund, especially at Seokmo-Ri Ga.

3.4 Sources contributing to surface O_3 in continental South Africa

As indicated above (section 3.1), the O_3 peaks in continental South Africa usually reflect increased concentrations of precursor species from anthropogenic sources during winter, as well as the occurrence of regional open biomass burning in late winter and early spring. In addition, stratospheric O_3 intrusions during spring (Lefohn et al., 2014) could also partially contribute to increased surface O_3 levels.

3.4.1 Anthropogenic and open biomass burning emissions

A comparison of the O_3 seasonal cycles at background and polluted locations is useful for source attribution. From Fig. 3, it is evident that daytime O_3 levels peaked at Elandsfontein, Marikana and Welgegund during late winter and spring (August to October), while O_3 levels at Botsalano peaked later in the year during spring (September to November). This suggests that Elandsfontein, Marikana and Welgegund were influenced by increased levels of O_3 precursors from anthropogenic and open biomass burning emissions (i.e. NO_x and CO indicated in Fig. A4 and Fig. A5, respectively – time series plotted in Fig. A7 and A8), while O_3 levels at Botsalano were predominantly influenced by regional open biomass burning (Fig. A5). Although Welgegund and Botsalano are both background sites, Botsalano is more removed from anthropogenic source regions than Welgegund is (section 2.1.3), which is therefore not directly influenced by the increased concentrations of O_3 precursor species associated with anthropogenic emissions during winter. Daytime O_3 concentrations were the highest at Marikana throughout most of the year, which indicates the influence of local and regional sources of O_3 precursors at this site (Venter et al., 2012). In addition, a larger difference between O_3 concentrations in summer and winter/spring is observed at Marikana compared to Welgegund and Botsalano, which can be attributed to local anthropogenic emissions (mainly household combustion) of O_3 precursors at Marikana.

O_3 concentrations at Elandsfontein were lower compared to the other three sites throughout the year, with the exception of the winter months (June to August). The major point sources at Elandsfontein include NO_x emissions from coal-fired power stations and are characterised by high-stack emissions, which are emitted above the low-level night-time inversion layers. During day time, downwards mixing of these emitted species occurs, which results in daytime peaks of NO_x (as indicated in Fig. A4 and by Collett et al., 2010) and subsequent O_3 titration. In contrast,

Venter et al. (2012) indicated that, at Marikana, low-level emissions associated with household combustion for space heating and cooking were a significant source of O_3 precursor species, i.e. NO_x and CO. The diurnal pattern of NO_x and CO (Fig. A4 and Fig. A5, respectively) at Marikana was characterised by bimodal peaks during the morning and evening, which resulted in increased O_3 concentrations during daytime and night-time titration of O_3, especially during winter. Therefore, the observed differences in night-time titration at Marikana and Elandsfontein can be attributed to different sources of O_3 precursors, i.e. mainly low-level emissions (household combustion) at Marikana (Venter et al., 2012) compared to predominantly high-stack emissions at Elandsfontein (Collette et al., 2010). The higher O_3 concentrations at Elandsfontein during winter are most likely attributed to the regional increase in O_3 precursors.

The spring maximum O_3 concentrations can be attributed to increases in widespread regional biomass burning in this region during this period (Vakkari et al., 2014; Lourens et al., 2011). Biomass burning has strong seasonality in southern Africa, extending from June to September (Galanter et al., 2000), and is an important source of O_3 and its precursors during the dry season. In an effort to elucidate the influence of regional biomass burning on O_3 concentrations in continental South Africa, source area maps of O_3 were compiled by relating O_3 concentrations measured with air mass history, which are presented in Fig. 5 (a). Source area maps were only generated for the background sites Welgegund and Botsalano, since local sources at the industrial sites Elandsfontein and Marikana would obscure the influence of regional biomass burning. In addition, maps of spatial distribution of fires during 2007, 2010 and 2015 were compiled with the MODIS collection 5 burnt area product (Roy et al., 2008; Roy et al., 2005; Roy et al., 2002), which are presented in Fig. 6.

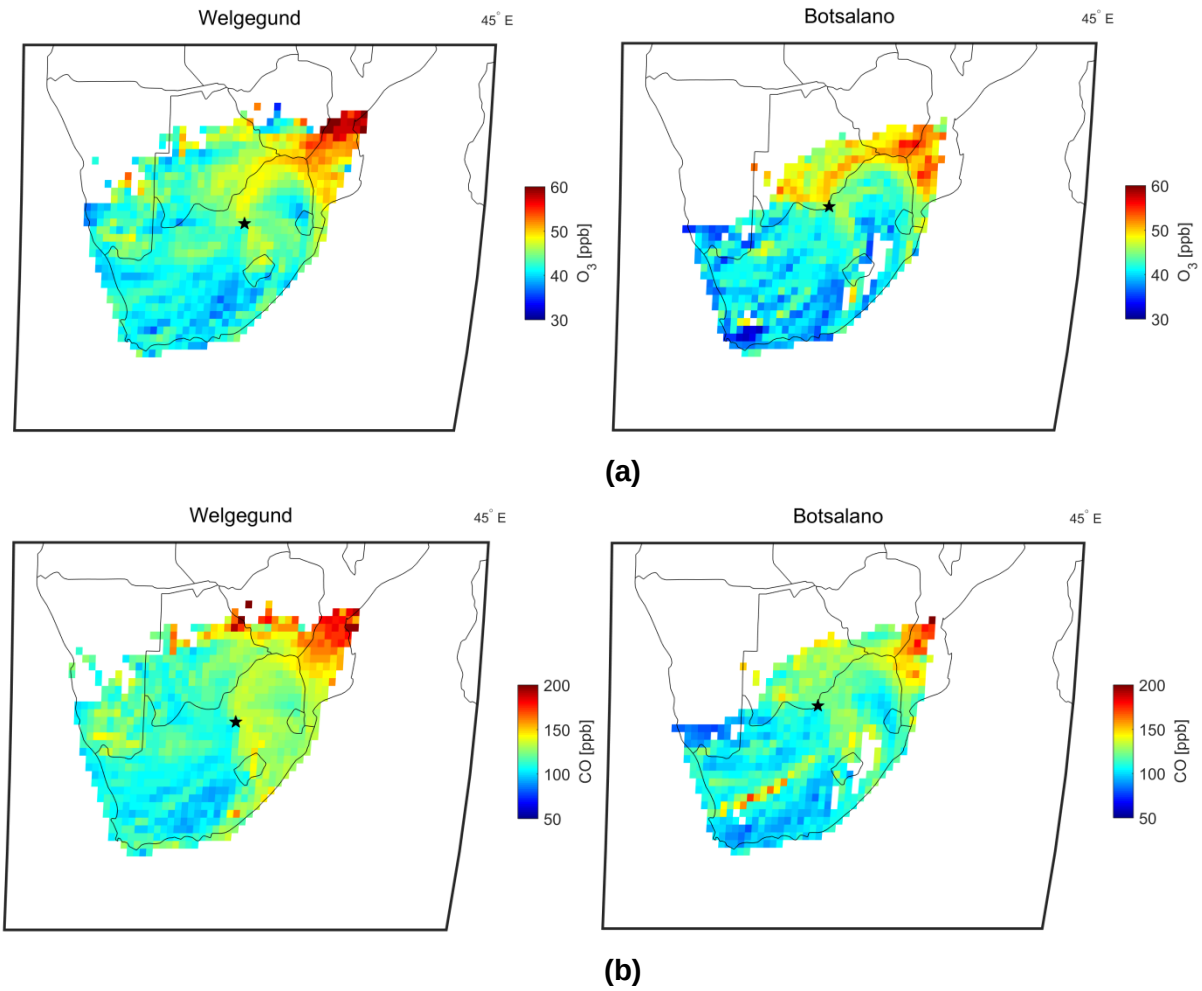

Fig. 5. Source area maps of (a) O_3 concentrations and (b) CO concentrations for the background sites Welgegund and Botsalano. The black star represents the measurement site and the colour of each pixel represents the mean concentration of the respective gas species. At least ten observations per pixel are required.

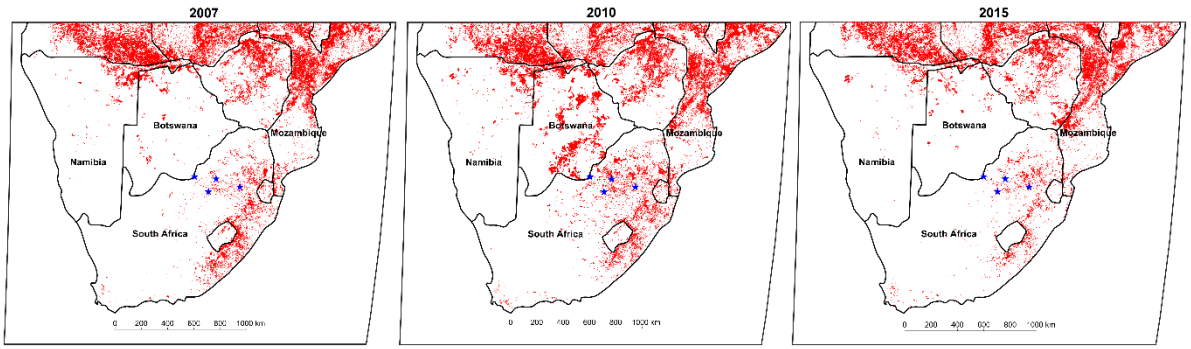

Fig. 7. Spatial distribution of fires in 2007, 2010 and 2015 from MODIS burnt area product. Blue stars indicate (from left to right) Botsalano, Welgegund, Marikana and Elandsfontein.

The highest O_3 concentrations measured at Welgegund and Marikana were associated with air masses passing over a sector north to north-east of these sites, i.e. southern and central Mozambique, southern Zimbabwe and south-eastern Botswana. O_3 concentrations associated with air masses passing over central and southern Mozambique were particularly high. In addition to O_3 source maps, CO source maps were also compiled for Welgegund and Botsalano, as indicated in Fig. 5 (b). It is evident that the CO source maps indicated a similar pattern than that observed for O_3 with the highest CO concentrations corresponding with the same regions where O_3 levels are the highest. From the fire maps in Fig. 6, it can be observed that a large number of fires occur in the sector, associated with higher O_3 and CO concentrations, with the fire map indicating, especially, a high fire frequency occurring in central Mozambique. During 2007, more fires occurred in Botswana compared to the other two years, which is also reflected in the higher O_3 levels measured at Botsalano during that year for air masses passing over this region. Open biomass burning is known to emit more CO than NO_x, while CO also has a relatively long atmospheric lifetime (1 to 2 months, Kanakidou and Crutzen, 1999) compared to NO_x (6 to 24 hours, Beirle et al., 2003) and VOCs (few hours to a few weeks, Kanakidou and Crutzen, 1999) emitted from open biomass burning. Enhanced CO concentrations have been used previously to characterise the dispersion of biomass burning emissions over southern Africa (Mafusire et al., 2016). Therefore, the regional transport of CO and VOCs (and NO_x to a lesser extent) associated with biomass burning occurring from June to September in southern Africa can be considered an important source of surface O_3 in continental South Africa (Fig. A5).

3.4.2 Stratospheric O_3

Elevated levels of tropospheric O_3 may also be caused by stratospheric intrusion of O_3-rich air (Zhang et al., 2014; Parrish et al., 2013; Lin et al., 2012), especially on certain days during late winter and spring when O_3 is the highest on the South African Highveld (Thompson et al., 2014). However, the importance of the stratospheric source over continental South Africa has not yet been specifically addressed. The assessment of meteorological fields and air quality data at high-elevation sites is required to determine the downward transport of stratospheric O_3. Alternatively, stratospheric O_3 intrusions can be estimated through concurrent in-situ measurements of ground-level O_3, CO and humidity, since stratospheric intrusions of O_3 into the troposphere are characterised by elevated levels of O_3, high potential vorticity, low levels of CO and low water vapour (Stauffer et al., 2017; Thompson et al., 2015; Thompson et al., 2014). Thompson et al. (2015) defined low CO as 80 to 110 ppbv, while low relative humidity (RH) is considered <15 %. In Fig. 7, the 95th percentile O_3 levels (indicative of "high O_3") corresponding to low daily average CO concentrations (< 100 ppb) are presented together with the daily average RH. Only daytime data from 07:00 to 18:00 (LT) was considered in order to exclude the influence of night-time titration. From Fig. 7, it is evident that very few days complied with the criteria indicative of stratospheric O_3 intrusion, i.e. high O_3, low CO and low RH, which indicates a very small influence of stratospheric intrusion on surface O_3 levels. However, it must be noted that the attempt in this study to relate surface O_3 to stratospheric intrusions is a simplified qualitative assessment and more quantitative detection methods should be applied to understand the influence of stratospheric intrusions on surface O_3 for this region.

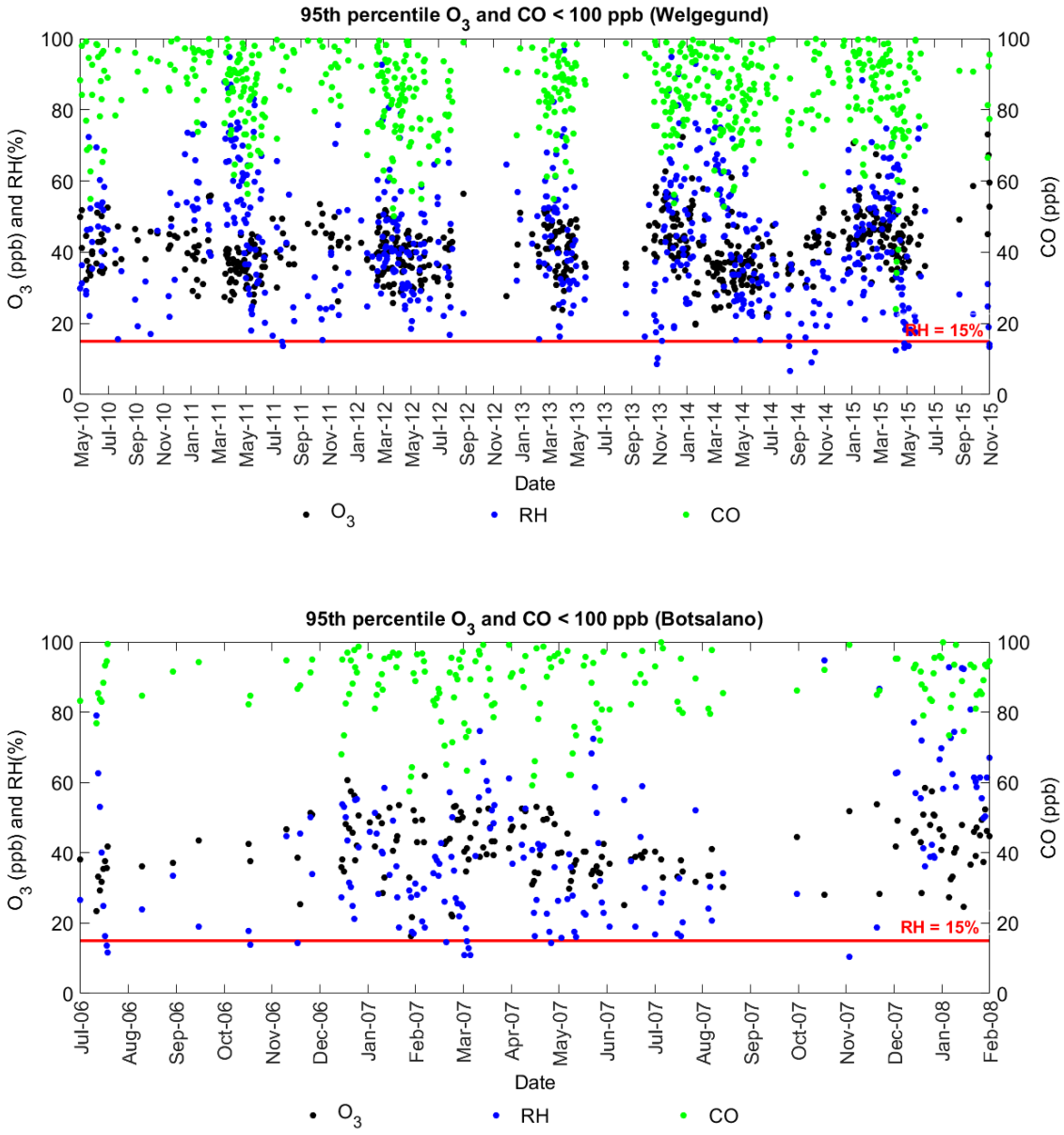

Fig. 7. Simultaneous measurements of O_3 (daily 95th percentile), CO (daily average ppb) and RH (daily average) from 07:00 to 18:00 LT at Welgegund, Botsalano and Marikana.

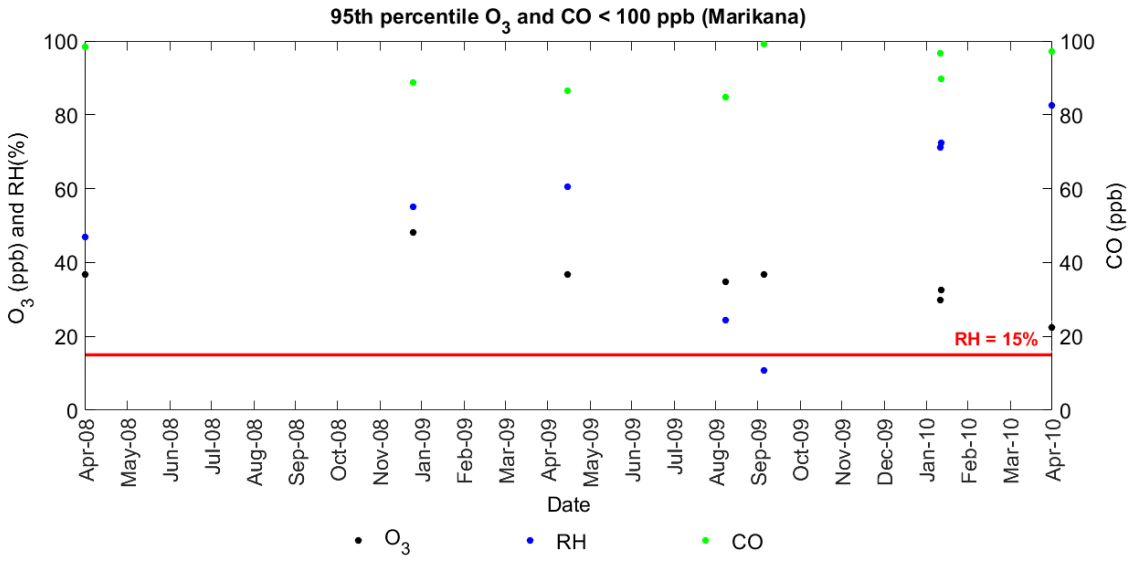

Fig. 7. Continued.

3.5 Insights into the O_3 production regime

The relationship between O_3, NO_x and CO was used as an indicator to infer the O_3 production regime at Welgegund, Botsalano and Marikana (no CO measurements were conducted at Elandsfontein as indicated above), since no continuous VOC measurements were conducted at each of these sites. However, as indicated in Section 2.4, a two-year VOC dataset was available for Welgegund (Jaars et al., 2016; Jaars et al., 2014), which was used to calculate the instantaneous production rate of O_3 as a function of NO_2 levels and VOC reactivity (Geddes et al., 2009; Murphy et al., 2006).

3.5.1 The relationship between NO_x, CO and O_3

In Fig. 8, the correlations between O_3, NO_x and CO concentrations at Welgegund, Botsalano and Marikana are presented, which clearly indicate higher O_3 concentrations associated with increased CO levels, while O_3 levels remain relatively constant (or decrease) with increasing NO_x. The highest O_3 concentrations occur for NO_x levels below 10 ppb, since the equilibrium between photochemical production of O_3 and chemical removal of O_3 shifts towards the former, i.e. greater O_3 formation. In general, there seems to exist a marginal negative correlation between O_3 and NO_x (Fig. A6) at all four sites, which is a reflection of the photochemical production of O_3 from

NO_2 and the destruction of O_3 through NO_x titration. These correlations between NO_x, CO and O_3 indicate that O_3 production in continental South Africa is limited by CO (and VOCs) concentrations, i.e. VOC-limited.

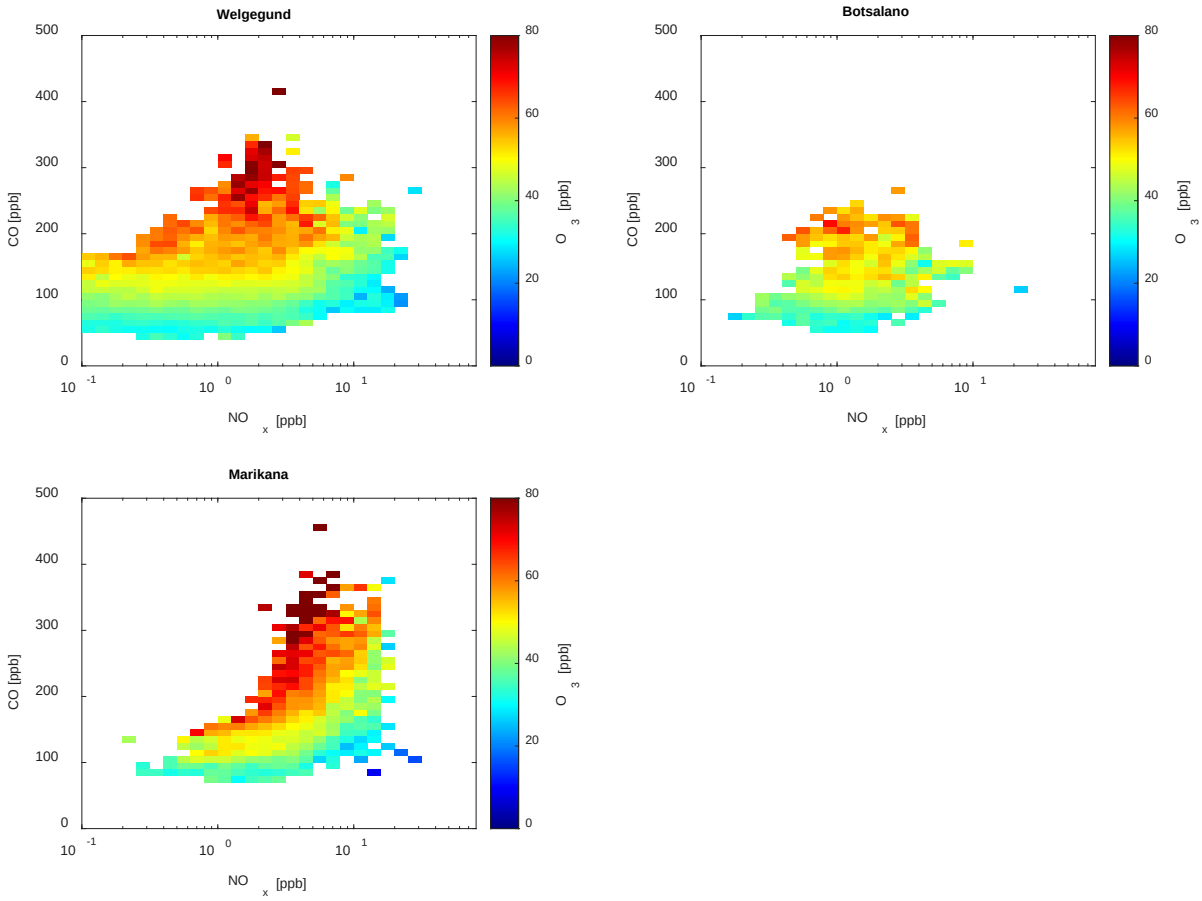

Fig. 8. Mean O_3 concentration averaged for NO_x and CO bins. Measurements were only taken from 11:00 to 17:00 LT when photochemical production of O_3 is at a maximum.

This finding shows a strong correlation between O_3 on CO and suggests that high O_3 can be attributed to the oxidation of CO in the air masses, i.e. as long as there is a sufficient amount of NO_x present in a region, CO serves to produce O_3. Although NO_x and VOCs are usually considered as the main precursors in ground-level O_3 formation, CO acts together with NO_x and VOCs in the presence of sunlight to drive photochemical O_3 formation. According to Fig. 8, reducing CO emissions should result in a reduction in surface O_3 and it is assumed that this response is analogous to that of VOCs. It is, however, not that simple, since the ambient NO_x and VOCs concentrations are directly related to the instantaneous rate of production of O_3 and not necessarily to the ambient O_3 concentration at a location, which is the result of chemistry,

deposition and transport that have occurred over several hours or a few days (Sillman, 1999). Notwithstanding the various factors contributing to increased surface O_3 levels, the correlation between ambient CO and O_3 is especially relevant given the low reactivity of CO with respect to $^{\bullet}OH$ radicals compared to most VOCs, which implies that the oxidation of CO probably takes place over a timescale of several days. It seems that the role of CO is of major importance in tropospheric chemistry in this region, where sufficient NO_x is present across continental South Africa and biogenic VOCs are relatively less abundant (Jaars et al., 2016), to fuel the O_3 formation process.

3.5.2 Seasonal change in O_3-precursors relationship

Seasonal changes in the relationship between O_3 and precursor species can be indicative of different sources of precursor species during different times of the year. In Fig. 9, the correlations between O_3 levels with NO_x and CO are presented for the different seasons, which indicate seasonal changes in the dependence of elevated O_3 concentrations on these precursors. The very high CO concentrations relative to NO_x, i.e. high CO to NO_x ratios, are associated with the highest O_3 concentrations, which are most pronounced (highest CO/NO_x ratios) during winter and spring. This indicates that the winter and spring O_3 maximum is primarily driven by increased peroxy radical production from CO and VOCs. The seasonal maximum in O_3 concentration coincides with the maximum CO concentration at the background sites, while the O_3 peak occurs just after June/July when CO peaked at the polluted site Marikana (Fig. A5). This observed seasonality in O_3 production signifies the importance of precursor species emissions from open biomass burning during winter and spring in this region, while household combustion for space heating and cooking is also an important source of O_3 precursors, as previously discussed. The strong diurnal CO concentration patterns observed during winter at Marikana (Fig. A5) substantiate the influence of household combustion on CO levels as indicated by Venter et al. (2012).

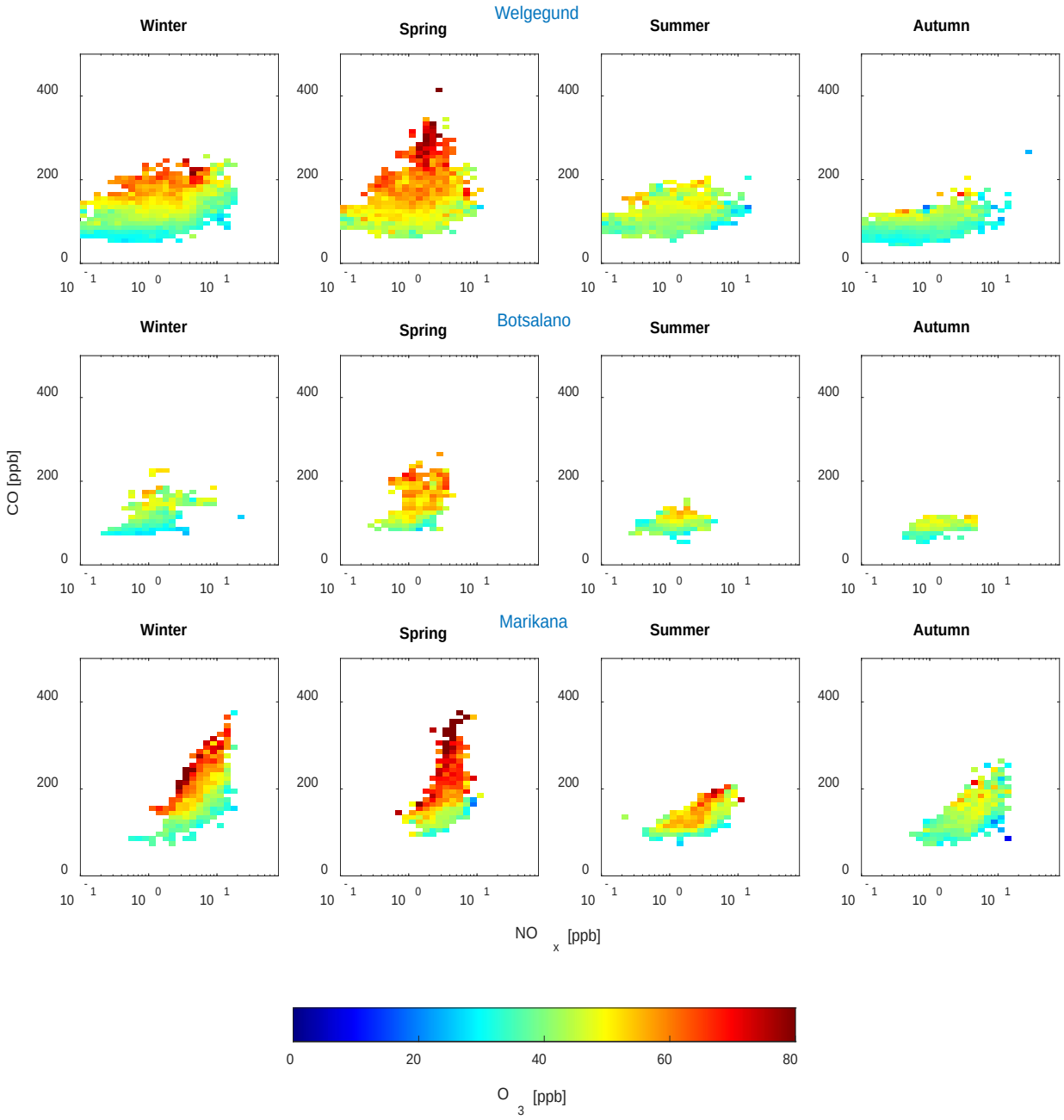

Fig. 9. Seasonal plots of the relationship between O_3, NO_x and CO at Welgegund, Botsalano and Marikana.

3.5.3 O_3 production rate

In Fig. 10, $P(O_3)$ as a function of VOC reactivity calculated from the available VOC dataset for Welgegund (Section 2.4) and NO_2 concentrations is presented. O_3 production at Welgegund during two field campaigns, specifically at 11:00 LT, was found to range between 0 and 10 ppbv

h^{-1}. The average $P(O_3)$ over the 2011 to 2012 and the 2014 to 2015 campaigns combined were 3.0 ± 1.9 ppbv h^{-1} and 3.2 ± 3.0 ppbv h^{-1}, respectively. The dashed black line in Fig. 10, called the ridge line, separates the NO_x- and VOC-limited regimes. To the left of the ridge line is the NO_x-limited regime, when O_3 production increases with increasing NO_x concentrations. The VOC-limited regime is to the right of the ridge line, when O_3 production decreases with increasing NO_x. According to the O_3 production plot presented, approximately 40% of the data is found in the VOC-limited regime area, which would support the regional O_3 analysis conducted for continental South Africa in this study. However, the O_3 production plot for Welgegund transitions between NO_x- and VOC-limited regimes, with Welgegund being in a NO_x-limited production regime the majority of the time, especially when NO_x concentrations are very low (<1 ppb). As indicated in section 2.4, limitations to this analysis include limited VOC speciation data, as well as a single time-of-day grab sample. The O_3 production rates can therefore only be inferred at 11:00 am LT despite O_3 concentrations peaking during the afternoon at Welgegund. Therefore, clean background air O_3 production is most-likely NO_x-limited (Tiitta et al., 2014), while large parts of the regional background of continental South Africa can be considered VOC-limited.

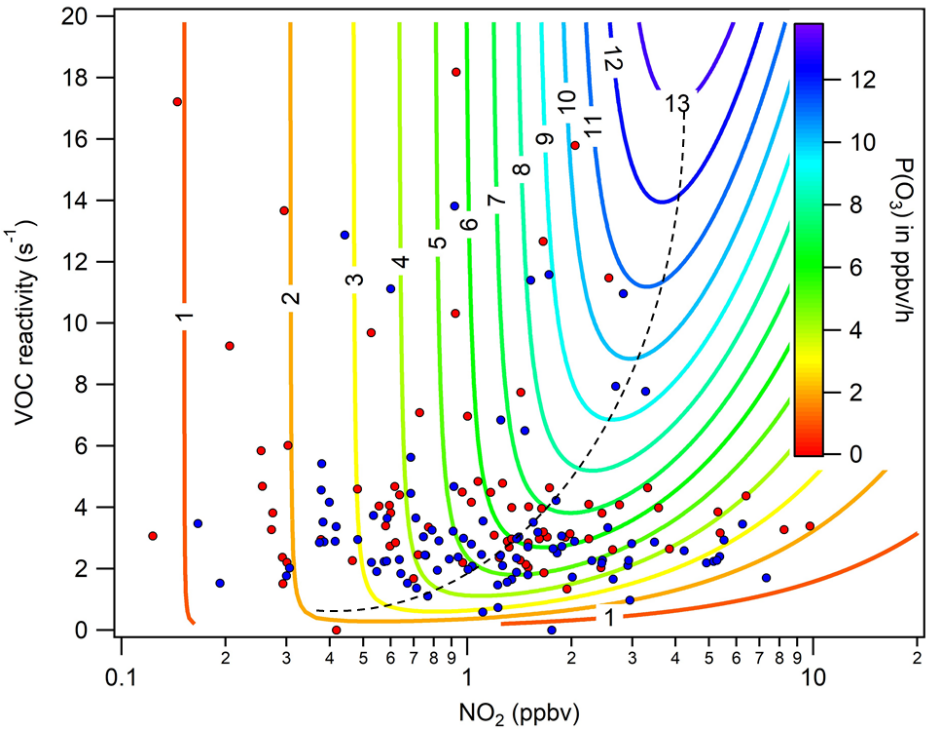

Fig. 10. Contour plot of instantaneous O_3 production ($P(O_3)$) at Welgegund using daytime (11:00 LT) grab sample measurements of VOCs and NO_2. The blue dots represent the first campaign (2011-2012), and the red dots indicate the second campaign (2014-2015).

3.6 Implications for air quality management

3.6.1 Ozone exceedances

The South African National Ambient Air Quality Standard (NAAQS) for O_3 is an eight-hour moving average limit of 61 ppbv with 11 exceedances allowed annually (Government Gazette Republic of South Africa, 2009). Fig. 11 shows the average number of days per month when this O_3 standard limit was exceeded at the four measurement sites. It is evident that the daily eight-h-O_3-maximum concentrations regularly exceeded the NAAQS threshold for O_3 and the number of exceedances annually allowed at all the sites, including the most remote of the four sites, Botsalano. At the polluted locations of Marikana and Elandsfontein, the O_3 exceedances peak early on in the dry season (June onwards), while at the background locations of Welgegund and Botsalano, the highest numbers of exceedances occur later in the dry season (August to November). These relatively high numbers of O_3 exceedances at all the sites (background and industrial) highlight the regional O_3 problem in South Africa, with background sites being impacted by the regional transport of O_3 precursors from anthropogenic and biomass burning source regions.

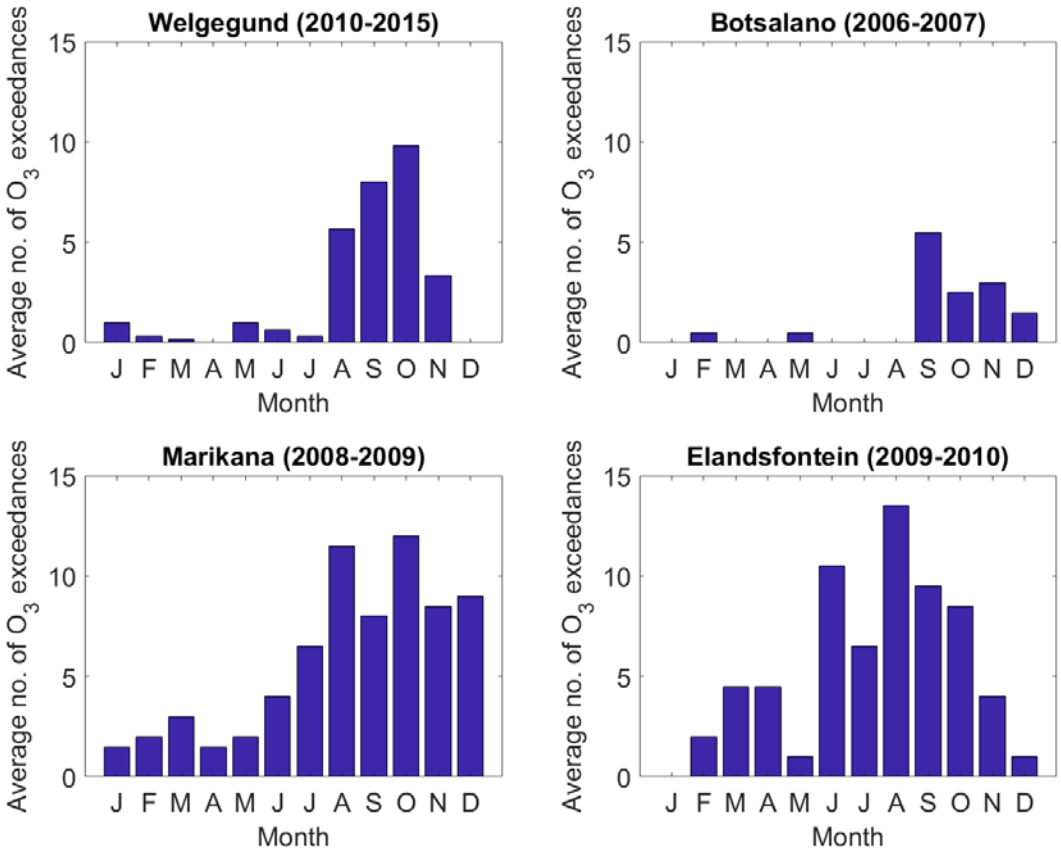

Fig. 11. Monthly number of exceedances of the daily 8-h-O_3-max (i.e. highest value of all available 8-hour moving averages in that day) above 61 ppbv at Welgegund, Botsalano, Marikana and Elandsfontein.

3.6.2 O_3 control strategies

As indicated above (sections 3.4 and 3.5), O_3 formation in the regions where Welgegund, Botsalano and Marikana are located can be considered VOC-limited, while the highly industrialised region with high NO_x emissions where Elandsfontein is located could also be considered VOC-limited. Rural remote regions are generally considered to be NO_x-limited due to the availability of NO_x and the impact of BVOCs (Sillman, 1999). However, Jaars et al. (2016) indicated that BVOC concentrations at a savannah grassland were at least an order of magnitude lower compared to other regions in the world. Therefore, very low BVOC concentrations, together with high anthropogenic emissions of NO_x in the interior of South Africa, result in VOC-limited conditions at background sites in continental South Africa.

It is evident that reducing CO- and VOC concentrations associated with anthropogenic emissions, e.g. household combustion, vehicular emissions and industries, would be the most efficient control strategy to reduce peak O_3 concentrations in the interior of South Africa. It is also imperative to consider the seasonal variation in the CO and VOC source strength in managing O_3 pollution in continental southern Africa. This study also revealed the significant contribution of biomass burning to O_3 precursors in this region, which should also be considered when implementing O_3 control strategies. However, since open biomass burning in southern Africa is of anthropogenic and natural origin, while O_3 concentrations in continental South Africa are also influenced by trans boundary transport of O_3 precursors from open biomass burning occurring in other countries in southern Africa (as indicated above), it is more difficult to control. Nevertheless, open biomass burning caused by anthropogenic practices (e.g. crop residue, pasture maintenance fires, opening burning of garbage) can be addressed.

4. Conclusions

A spatial distribution map of O_3 levels in the interior of South Africa indicated the regional O_3 problem in continental South Africa, which was signified by the regular exceedance of the South African air quality standard limit. The seasonal and diurnal O_3 patterns observed at the four sites in this study resembled typical trends for O_3 in continental South Africa, with O_3 concentrations peaking in late winter and early spring (cf. Zunckel et al., 2004), while daytime O_3 corresponded to increased photochemical production. The seasonal O_3 trends observed in continental southern Africa could mainly be attributed to the seasonal changes in emissions of O_3 precursor species and local meteorological conditions. Increased O_3 concentrations in winter at Welgegund, Marikana and Elandsfontein reflected increased household combustion for space heating and the trapping of low-level pollutants near the surface. A spring maximum observed at all the sites was attributed to increased regional open biomass burning. Significantly higher O_3 concentrations, which corresponded with increased CO concentrations, were associated with air masses passing over a region in southern Africa, where a large number of open biomass burning occurred from June to September. Therefore, the regional transport of CO associated with open biomass burning in southern Africa was considered a significant source of surface O_3 in continental South Africa. A very small contribution from the stratospheric intrusion of O_3-rich air to surface O_3 levels at the four sites was indicated.

The relationship between O_3, NO_x and CO at Welgegund, Botsalano and Marikana indicated a strong correlation between O_3 on CO, while O_3 levels remained relatively constant (or decreased) with increasing NO_x. Although NO_x and VOCs are usually considered to be the main precursors in ground-level O_3 formation, CO can also drive photochemical O_3 formation. The seasonal changes in the relationship between O_3 and precursors species also reflected the higher CO emissions associated with increased household combustion in winter, and open biomass burning in late winter and spring. The calculation of the $P(O_3)$ from a two-year VOC dataset at Welgegund indicated that at least 40% of O_3 production occurred in the VOC-limited regime. These results indicated that large parts in continental South Africa can be considered VOC-limited, which can be attributed to high anthropogenic emissions of NO_x in this region. It is, however, recommended that future studies should investigate more detailed relationships between NO_x, CO, VOCs and O_3 through photochemical modelling analysis, while concurrent measurement of atmospheric VOCs and $^{\bullet}OH$ would also contribute to the better understanding of surface O_3 in this region.

In this paper, some new aspects on O_3 for continental South Africa have been indicated, which must be taken into consideration when O_3 mitigation strategies are deployed. Emissions of O_3 precursor species associated with the concentrated location of industries in this area could be regulated, while CO and VOC emissions associated with household combustion and regional open biomass burning should also be targeted. However, emissions of O_3 precursor species related to factors such as household combustion associated with poor socio-economic circumstances and long-range transport provide a bigger challenge for regulators.

Acknowledgements

The financial assistance of the National Research Foundation (NRF) towards this research is hereby acknowledged. Opinions expressed and conclusions arrived at are those of the authors and are not necessarily to be attributed to the NRF. We thank the Tropospheric Ozone Assessment Report (TOAR) initiative for providing the surface ozone data used in this publication. The authors are also grateful to Eskom for supplying the Elandsfontein data. Thanks are also due to Dirk Cilliers from the NWU for the GIS assistance. V Vakkari is a beneficiary of an AXA Research Fund postdoctoral grant. This work was partly funded by the Academy of Finland Centre of Excellence program (grant no. 272041).

5. References

Air Resources Laboratory: Gridded Meteorological Data Archives, available at: https://www.ready.noaa.gov/archives.php, 2017.

Atkinson, R.: Atmospheric chemistry of VOCs and NO_x, Atmospheric Environment, 34, 2063-2101, 2000.

Atlas, E. L., Ridley, B. A., and Cantrell, C. A.: The Tropospheric Ozone Production about the Spring Equinox (TOPSE) Experiment: Introduction, Journal of Geophysical Research: Atmospheres, 108, n/a-n/a, doi:10.1029/2002JD003172, 2003.

Balashov, N. V., Thompson, A. M., Piketh, S. J., and Langerman, K. E.: Surface ozone variability and trends over the South African Highveld from 1990 to 2007, Journal of Geophysical Research: Atmospheres, 119, 4323-4342, doi:10.1002/2013JD020555, 2014.

Beirle, S., Platt, U., Wenig, M., and Wagner, T.: Weekly cycle of NO 2 by GOME measurements: A signature of anthropogenic sources, Atmospheric Chemistry and Physics, 3, 2225-2232, 2003.

Carvalho, A., Monteiro, A., Ribeiro, I., Tchepel, O., Miranda, A. I., Borrego, C., Saavedra, S., Souto, J. A., and Casares, J. J.: High ozone levels in the northeast of Portugal: Analysis and characterization, Atmospheric Environment, 44, 1020-1031, doi:http://dx.doi.org/10.1016/j.atmosenv.2009.12.020, 2010.

Cazorla, M., and Brune, W. H.: Measurement of Ozone Production Sensor, Atmos. Meas. Tech., 3, 545-555, doi:10.5194/amt-3-545-2010, 2010.

Chevalier, A., Gheusi, F., Delmas, R., Ordóñez, C., Sarrat, C., Zbinden, R., Thouret, V., Athier, G., and Cousin, J. M.: Influence of altitude on ozone levels and variability in the lower troposphere: a ground-based study for western Europe over the period 2001-2004, Atmos. Chem. Phys., 7, 4311-4326, doi:10.5194/acp-7-4311-2007, 2007.

Collett, K. S., Piketh, S. J., and Ross, K. E.: An assessment of the atmospheric nitrogen budget on the South African Highveld, South African Journal of Science, doi:10.4102/sajs.v106i5/6.220, 2010.

Cooper, O. R., Gao, R. S., Tarasick, D., Leblanc, T., and Sweeney, C.: Long-term ozone trends at rural ozone monitoring sites across the United States, 1990-2010, Journal of Geophysical Research: Atmospheres, 117, 2012.

Cooper, O. R., Parrish, D., Ziemke, J., Balashov, N., Cupeiro, M., Galbally, I., Gilge, S., Horowitz, L., Jensen, N., and Lamarque, J.-F.: Global distribution and trends of tropospheric ozone: An observation-based review, Elementa: Science of the Anthropocene, 2, 2014.

Crutzen, P. J., and Andreae, M. O.: Biomass Burning in the Tropics: Impact on Atmospheric Chemistry and Biogeochemical Cycles, Science, 250, 1669-1678, doi:10.1126/science.250.4988.1669, 1990.

Crutzen, P. J., Lawrence, M. G., and PÖSchl, U.: On the background photochemistry of tropospheric ozone, Tellus B, 51, 123-146, doi:10.1034/j.1600-0889.1999.00010.x, 1999.

Diab, R., Thompson, A., Mari, K., Ramsay, L., and Coetzee, G.: Tropospheric ozone climatology over Irene, South Africa, from 1990 to 1994 and 1998 to 2002, Journal of Geophysical Research: Atmospheres, 109, 2004.

Diab, R. D., Thompson, A. M., Zunckel, M., Coetzee, G. J. R., Combrink, J., Bodeker, G. E., Fishman, J., Sokolic, F., McNamara, D. P., Archer, C. B., and Nganga, D.: Vertical ozone distribution over southern Africa and adjacent oceans during SAFARI-92, Journal of Geophysical Research: Atmospheres, 101, 23823-23833, doi:10.1029/96JD01267, 1996.

Draxler, R. R., and Hess, G. D.: An overview of the HYSPLIT_4 modeling system of trajectories, dispersion, and deposition, Aystralian Meteorological Magazine, 47, 295-308, 1998.

Dueñas, C., Fernández, M. C., Cañete, S., Carretero, J., and Liger, E.: Assessment of ozone variations and meteorological effects in an urban area in the Mediterranean Coast, Science of The Total Environment, 299, 97-113, doi:https://doi.org/10.1016/S0048-9697(02)00251-6, 2002.

Dyson, L. L., Van Heerden, J., and Sumner, P. D.: A baseline climatology of sounding-derived parameters associated with heavy rainfall over Gauteng, South Africa, International Journal of Climatology, 35, 114-127, 2015.

Galanter, M., Levy, H., and Carmichael, G. R.: Impacts of biomass burning on tropospheric CO, NO_x, and O_3, Journal of Geophysical Research: Atmospheres, 105, 6633-6653, 2000.

Garstang, M., Tyson, P. D., Swap, R., Edwards, M., Kållberg, P., and Lindesay, J. A.: Horizontal and vertical transport of air over southern Africa, Journal of Geophysical Research: Atmospheres, 101, 23721-23736, doi:10.1029/95JD00844, 1996.

Geddes, J. A., Murphy, J. G., and Wang, D. K.: Long term changes in nitrogen oxides and volatile organic compounds in Toronto and the challenges facing local ozone control, Atmospheric Environment, 43, 3407-3415, doi:https://doi.org/10.1016/j.atmosenv.2009.03.053, 2009.

Held, G., Scheifinger, H., Snyman, G., Tosen, G., and Zunckel, M.: The climatology and meteorology of the Highveld, Air pollution and its impacts on the South African Highveld. Johannesburg: Environmental Scientific Association, 60-71, 1996.

Hirsikko, A., Vakkari, V., Tiitta, P., Manninen, H. E., Gagné, S., Laakso, H., Kulmala, M., Mirme, A., Mirme, S., Mabaso, D., Beukes, J. P., and Laakso, L.: Characterisation of sub-micron particle number concentrations and formation events in the western Bushveld Igneous Complex, South Africa, Atmospheric Chemistry and Physics, 12, 3951-3967, doi:10.5194/acp-12-3951-2012, 2012.

Hirsikko, A., Vakkari, V., Tiitta, P., Hatakka, J., Kerminen, V. M., Sundström, A. M., Beukes, J. P., Manninen, H. E., Kulmala, M., and Laakso, L.: Multiple daytime nucleation events in semi-clean savannah and industrial environments in South Africa: analysis based on observations, Atmospheric Chemistry and Physics., 13, 5523-5532, doi:10.5194/acp-13-5523-2013, 2013.

Holloway, A. M., and Wayne, R. P.: Atmospheric chemistry, Royal Society of Chemistry, Cambridge, xiii, 271 p. pp., 2010.

IPCC: Climate change 2013: The physical science basis: contribution of Working Group I to the Fifth Assessment Report of the Intergovernmental Panel on Climate Change, edited by: Stocker, T. F., Qin, D., Plattner, G.-K., Tignor, M., Allen, S. K., Boschung, J., Nauels, A., Xia, Y., Bex, B., and Midgley, B., Cambridge University Press, 2013.

Jaars, K., Beukes, J. P., van Zyl, P. G., Venter, A. D., Josipovic, M., Pienaar, J. J., Vakkari, V., Aaltonen, H., Laakso, H., Kulmala, M., Tiitta, P., Guenther, A., Hellén, H., Laakso, L., and Hakola, H.: Ambient aromatic hydrocarbon measurements at Welgegund, South Africa, Atmospheric Chemistry and Physics., 14, 7075-7089, doi:10.5194/acp-14-7075-2014, 2014.

Jaars, K., van Zyl, P. G., Beukes, J. P., Hellén, H., Vakkari, V., Josipovic, M., Venter, A. D., Räsänen, M., Knoetze, L., Cilliers, D. P., Siebert, S. J., Kulmala, M., Rinne, J., Guenther, A., Laakso, L., and Hakola, H.: Measurements of biogenic volatile organic compounds at a grazed savannah grassland agricultural landscape in South Africa, Atmospheric Chemistry and Physics, 16, 15665-15688, doi:10.5194/acp-16-15665-2016, 2016.

Jaeglé, L., Jacob, D.J., Brune, W.H., Wennberg, P.O., Chemistry of HO_x radicals in the upper troposphere, Atmospheric Environment, 35 (3), 469-489, https://doi.org/10.1016/S1352-2310(00)00376-9, 2001

Josipovic, M.: Acidic deposition emanating from the South African Highveld: A critical levels and critical loads assessment (PhD thesis), University of Johannesburg, 2009.

Josipovic, M., Annegarn, H. J., Kneen, M. A., Pienaar, J. J., and Piketh, S. J.: Concentrations, distributions and critical level exceedance assessment of SO_2, NO_2 and O_3 in South Africa, Environmental Monitoring and Assessment, 171, 181-196, doi:10.1007/s10661-009-1270-5, 2010.

Kanakidou, M., and Crutzen, P. J.: The photochemical source of carbon monoxide: Importance, uncertainties and feedbacks, Chemosphere-Global Change Science, 1, 91-109, 1999.

Klopper, E., Vogel, C. H., and Landman, W. A.: Seasonal climate forecasts–potential agricultural-risk management tools?, Climatic Change, 76, 73-90, 2006.

Laakso, L., Laakso, H., Aalto, P. P., Keronen, P., Petäjä, T., Nieminen, T., Pohja, T., Siivola, E., Kulmala, M., Kgabi, N., Molefe, M., Mabaso, D., Phalatse, D., Pienaar, K., and Kerminen, V. M.: Basic characteristics of atmospheric particles, trace gases and meteorology in a relatively clean Southern African Savannah environment, Atmospheric Chemistry and Physics, 8, 4823-4839, doi:10.5194/acp-8-4823-2008, 2008.

Laakso, L., Vakkari, V., Virkkula, A., Laakso, H., Backman, J., Kulmala, M., Beukes, J. P., van Zyl, P. G., Tiitta, P., Josipovic, M., Pienaar, J. J., Chiloane, K., Gilardoni, S., Vignati, E., Wiedensohler, A., Tuch, T., Birmili, W., Piketh, S., Collett, K., Fourie, G. D., Komppula, M., Lihavainen, H., de Leeuw, G., and Kerminen, V. M.: South African EUCAARI measurements: seasonal variation of trace gases and aerosol optical properties, Atmospheric Chemistry and Physics, 12, 1847-1864, doi:10.5194/acp-12-1847-2012, 2012.

Laakso, L., Beukes, J. P., Van Zyl, P. G., Pienaar, J. J., Josipovic, M., Venter, A. D., Jaars, K., Vakkari, V., Labuschagne, C., Chiloane, K., and Tuovinen, J.-P.: Ozone concentrations and their potential impacts on vegetation in southern Africa, in: Climate change, air pollution and global challenges understanding and perspectives from forest research, edited by: Matyssek, R., Clarke, N., Cudlin, P., Mikkelsen, T. N., Tuovinen, J.-P., Wieser, G., and Paoletti, E., 1 online resource (647 pages), 2013.

Lefohn, A. S., Emery, C., Shadwick, D., Wernli, H., Jung, J., and Oltmans, S. J.: Estimates of background surface ozone concentrations in the United States based on model-derived source apportionment, Atmospheric Environment, 84, 275-288, doi:https://doi.org/10.1016/j.atmosenv.2013.11.033, 2014.

Lin, M., Fiore, A. M., Cooper, O. R., Horowitz, L. W., Langford, A. O., Levy, H., Johnson, B. J., Naik, V., Oltmans, S. J., and Senff, C. J.: Springtime high surface ozone events over the western United States: Quantifying the role of stratospheric intrusions, Journal of Geophysical Research: Atmospheres, 117, n/a-n/a, doi:10.1029/2012JD018151, 2012.

Logan, J. A.: Tropospheric ozone: Seasonal behavior, trends, and anthropogenic influence, Journal of Geophysical Research: Atmospheres, 90, 10463-10482, doi:10.1029/JD090iD06p10463, 1985.

Lourens, A. S., Beukes, J. P., Van Zyl, P. G., Fourie, G. D., Burger, J. W., Pienaar, J. J., Read, C. E., and Jordaan, J. H.: Spatial and temporal assessment of gaseous pollutants in the Highveld of South Africa, South African Journal of Science, 107, 1-8, 2011.

Lourens, A. S. M., Butler, T. M., Beukes, J. P., Van Zyl, P. G., Beirle, S., Wagner, T. K., Heue, K.-P., Pienaar, J. J., Fourie, G. D., and Lawrence, M. G.: Re-evaluating the NO_2 hotspot over the South African Highveld, doi:10.4102/sajs.v108i11/12.1146, 2012.

Lourens, A. S. M., Butler, T. M., Beukes, J. P., Van Zyl, P. G., Fourie, G. D., and Lawrence, M. G.: Investigating atmospheric photochemistry in the Johannesburg-Pretoria megacity using a box model, South African Journal of Science, 112, 1-11, doi:http://dx.doi.org/10.17159/sajs.2016/2015-0169, 2016.

Macdonald, A. M., Anlauf, K. G., Leaitch, W. R., Chan, E., and Tarasick, D. W.: Interannual variability of ozone and carbon monoxide at the Whistler high elevation site: 2002-2006, Atmospheric Chemistry and Physics, 11, 11431-11446, doi:10.5194/acp-11-11431-2011, 2011.

Mafusire, G., Annegarn, H. J., Vakkari, V., Beukes, J. P., Josipovic, M., Van Zyl, P. G., and Laakso, L.: Submicrometer aerosols and excess CO as tracers for biomass burning air mass transport over southern Africa, Journal of Geophysical Research: Atmospheres, 121, 10262-10282, doi:10.1002/2015JD023965, 2016.

Monks, P. S., Archibald, A. T., Colette, A., Cooper, O., Coyle, M., Derwent, R., Fowler, D., Granier, C., Law, K. S., Mills, G. E., Stevenson, D. S., Tarasova, O., Thouret, V., von Schneidemesser, E., Sommariva, R., Wild, O., and Williams, M. L.: Tropospheric ozone and its precursors from the urban to the global scale from air quality to short-lived climate forcer, Atmospheric Chemistry and Physics, 15, 8889-8973, doi:10.5194/acp-15-8889-2015, 2015.

Murphy, J. G., Day, D. A., Cleary, P. A., Wooldridge, P. J., Millet, D. B., Goldstein, A. H., and Cohen, R. C.: The weekend effect within and downwind of Sacramento: Part 2. Observational evidence for chemical and dynamical contributions, Atmospheric Chemistry and Physics, Discuss., 2006, 11971-12019, doi:10.5194/acpd-6-11971-2006, 2006.

Novelli, P. C., Steele, L. P., and Tans, P. P.: Mixing ratios of carbon monoxide in the troposphere, Journal of Geophysical Research: Atmospheres, 97, 20731-20750, 1992.

NRC: Rethinking the Ozone Problem in Urban and Regional Air Pollution, The National Academies Press, Washington, DC, 524 pp., 1991.

Oltmans, S. J., Lefohn, A. S., Shadwick, D., Harris, J. M., Scheel, H. E., Galbally, I., Tarasick, D. W., Johnson, B. J., Brunke, E. G., Claude, H., Zeng, G., Nichol, S., Schmidlin, F., Davies, J., Cuevas, E., Redondas, A., Naoe, H., Nakano, T., and Kawasato, T.: Recent tropospheric ozone changes – A pattern dominated by slow or no growth, Atmospheric Environment, 67, 331-351, doi:https://doi.org/10.1016/j.atmosenv.2012.10.057, 2013.

Parrish, D. D., Law, K. S., Staehelin, J., Derwent, R., Cooper, O. R., Tanimoto, H., Volz-Thomas, A., Gilge, S., Scheel, H. E., Steinbacher, M., and Chan, E.: Lower tropospheric ozone at northern midlatitudes: Changing seasonal cycle, Geophysical Research Letters, 40, 1631-1636, doi:10.1002/grl.50303, 2013.

Petäjä, T., Vakkari, V., Pohja, T., Nieminen, T., Laakso, H., Aalto, P. P., Keronen, P., Siivola, E., Kerminen, V.-M., Kulmala, M., and Laakso, L.: Transportable Aerosol Characterization Trailer with Trace Gas Chemistry: Design, Instruments and Verification, Aerosol and Air Quality Research, 13, No. 2, 421-435, doi:10.4209/aaqr.2012.08.0207, 2013.

Roy, D., Lewis, P., and Justice, C.: Burned area mapping using multi-temporal moderate spatial resolution data: A bi-directional reflectance model-based expectation approach, Remote Sensing of Environment, 83, 263-286, 2002.

Roy, D., Frost, P., Justice, C., Landmann, T., Le Roux, J., Gumbo, K., Makungwa, S., Dunham, K., Du Toit, R., and Mhwandagara, K.: The Southern Africa Fire Network (SAFNet) regional burned-area product-validation protocol, International Journal of Remote Sensing, 26, 4265-4292, 2005.

Roy, D. P., Boschetti, L., Justice, C. O., and Ju, J.: The collection 5 MODIS burned area product: Global evaluation by comparison with the MODIS active fire product, Remote Sensing of Environment, 112, 3690-3707, 2008.

Schultz, M. G., Schröder, S., Lyapina, O., Cooper, O., Galbally, I., Petropavlovskikh, I., von Schneidemesser, E., Tanimoto, H., Elshorbany, Y., and Naja, M.: Tropospheric Ozone Assessment Report: Database and metrics data of global surface ozone observations, Elementa: Science of the Anthropocene, 5, doi:http://doi.org/10.1525/elementa.244, 2017.

Seinfeld, J. H., and Pandis, S. N.: Atmospheric chemistry and physics : from air pollution to climate change, Wiley-Interscience, New York ; Chichester, xxvii, 1326 p. pp., 1998.

Seinfeld, J. H., and Pandis, S. N.: Atmospheric chemistry and physics : from air pollution to climate change, 2nd ed., Wiley, New York, xxviii, 1202 p. pp., 2006.

Sillman, S.: The relation between ozone, NOx and hydrocarbons in urban and polluted rural environments, Atmospheric Environment, 33, 1821-1845, doi:http://dx.doi.org/10.1016/S1352-2310(98)00345-8, 1999.

Simpson, I. J., Akagi, S., Barletta, B., Blake, N., Choi, Y., Diskin, G., Fried, A., Fuelberg, H., Meinardi, S., and Rowland, F.: Boreal forest fire emissions in fresh Canadian smoke plumes: C1-C10 volatile organic compounds (VOCs), CO_2, CO, NO_2, NO, HCN and CH_3CN, Atmospheric Chemistry and Physics, 11, 6445-6463, 2011.

Srinivasan, N. K., Su, M.-C., Sutherland, J. W. and, and Michael, J. V., Reflected Shock Tube Studies of High-Temperature Rate Constants for OH + CH4 → CH3 + H2O and CH3 + NO2 → CH3O + NO, The Journal of Physical Chemistry A, 109 (9), 1857-1863, 2005, doi: 10.1021/jp040679j

Stauffer, R. M., Thompson, A. M., Oltmans, S. J., and Johnson, B. J.: Tropospheric ozonesonde profiles at long-term US monitoring sites: 2. Links between Trinidad Head, CA, profile clusters and inland surface ozone measurements, Journal of Geophysical Research: Atmospheres, 122, 1261-1280, 2017.

Stein, A. F., Draxler, R. R., Rolph, G. D., Stunder, B. J. B., Cohen, M. D., and Ngan, F.: NOAA's HYSPLIT Atmospheric Transport and Dispersion Modeling System, Bulletin of the American Meteorological Society, 96, 2059-2077, doi:10.1175/bams-d-14-00110.1, 2015.

Swap, R. J., Annegarn, H. J., Suttles, J. T., King, M. D., Platnick, S., Privette, J. L., and Scholes, R. J.: Africa burning: A thematic analysis of the Southern African Regional Science Initiative (SAFARI 2000), Journal of Geophysical Research: Atmospheres, 108, n/a-n/a, doi:10.1029/2003JD003747, 2003.

Thompson, A. M.: Biomass burning and the atmosphere: accomplishments and research opportunities, Atmospheric Environment, 30, i-ii, doi:https://doi.org/10.1016/S1352-2310(96)90021-7, 1996.

Thompson, A. M., Balashov, N. V., Witte, J. C., Coetzee, J. G. R., Thouret, V., and Posny, F.: Tropospheric ozone increases over the southern Africa region: bellwether for rapid growth in Southern Hemisphere pollution?, Atmospheric Chemistry and Physics, 14, 9855-9869, doi:10.5194/acp-14-9855-2014, 2014.

Thompson, A. M., Stauffer, R. M., Miller, S. K., Martins, D. K., Joseph, E., Weinheimer, A. J., and Diskin, G. S.: Ozone profiles in the Baltimore-Washington region (2006-2011): satellite comparisons and DISCOVER-AQ observations, Journal of atmospheric chemistry, 72, 393-422, 2015.

Tiitta, P., Vakkari, V., Croteau, P., Beukes, J. P., van Zyl, P. G., Josipovic, M., Venter, A. D., Jaars, K., Pienaar, J. J., Ng, N. L., Canagaratna, M. R., Jayne, J. T., Kerminen, V. M., Kokkola, H., Kulmala, M., Laaksonen, A., Worsnop, D. R., and Laakso, L.: Chemical composition, main sources and temporal variability of PM_1 aerosols in southern African grassland, Atmospheric Chemistry and Physics, 14, 1909-1927, doi:10.5194/acp-14-1909-2014, 2014.

Tyson, P. D., and Preston-Whyte, R. A.: The weather and climate of southern Africa, 2nd ed., xii, 396 pages pp., 2000.

Vakkari, V., Laakso, H., Kulmala, M., Laaksonen, A., Mabaso, D., Molefe, M., Kgabi, N., and Laakso, L.: New particle formation events in semi-clean South African savannah, Atmospheric Chemistry and Physics, 11, 3333-3346, doi:10.5194/acp-11-3333-2011, 2011.

Vakkari, V., Beukes, J. P., Laakso, H., Mabaso, D., Pienaar, J. J., Kulmala, M., and Laakso, L.: Long-term observations of aerosol size distributions in semi-clean and polluted savannah in South Africa, Atmospheric Chemistry and Physics, 13, 1751-1770, doi:10.5194/acp-13-1751-2013, 2013.

Vakkari, V., Kerminen, V.-M., Beukes, J. P., Tiitta, P., van Zyl, P. G., Josipovic, M., Venter, A. D., Jaars, K., Worsnop, D. R., Kulmala, M., and Laakso, L.: Rapid changes in biomass burning aerosols by atmospheric oxidation, Geophysical Research Letters, 41, 2644-2651, doi:10.1002/2014GL059396, 2014.

Venter, A. D., Vakkari, V., Beukes, J. P., Van Zyl, P. G., Laakso, H., Mabaso, D., Tiitta, P., Josipovic, M., Kulmala, M., Pienaar, J. J., and Laakso, L.: An air quality assessment in the industrialised western

Bushveld Igneous Complex, South Africa, South African Journal of Science, doi:10.4102/sajs.v108i9/10.1059, 2012.

Venter, A. D., van Zyl, P. G., Beukes, J. P., Josipovic, M., Hendriks, J., Vakkari, V., and Laakso, L.: Atmospheric trace metals measured at a regional background site (Welgegund) in South Africa, Atmospheric Chemistry and Physics, 17, 4251-4263, doi:10.5194/acp-17-4251-2017, 2017.

Vingarzan, R.: A review of surface ozone background levels and trends, Atmospheric Environment, 38, 3431-3442, doi:https://doi.org/10.1016/j.atmosenv.2004.03.030, 2004.

Wells, R., Lloyd, S., and Turner, C.: National air pollution source inventory, Air pollution and its impacts on the South African Highveld. Johannesburg: Environmental Scientific Association, 3-9, 1996.

Wilson, S. R.: Characterisation of $J(O^1D)$ at Cape Grim 2000–2005, Atmospheric Chemistry and Physics, 15, 7337-7349, https://doi.org/10.5194/acp-15-7337-2015, 2015

Yorks, J. E., Thompson, A. M., Joseph, E., and Miller, S. K.: The variability of free tropospheric ozone over Beltsville, Maryland (39N, 77W) in the summers 2004-2007, Atmospheric Environment, 43, 1827-1838, 2009.

Zhang, L., Jacob, D. J., Yue, X., Downey, N. V., Wood, D. A., and Blewitt, D.: Sources contributing to background surface ozone in the US Intermountain West, Atmospheric Chemistry and Physics, 14, 5295-5309, doi:10.5194/acp-14-5295-2014, 2014.

Zunckel, M., Venjonoka, K., Pienaar, J. J., Brunke, E. G., Pretorius, O., Koosialee, A., Raghunandan, A., and van Tienhoven, A. M.: Surface ozone over southern Africa: synthesis of monitoring results during the Cross border Air Pollution Impact Assessment project, Atmospheric Environment, 38, 6139-6147, doi:https://doi.org/10.1016/j.atmosenv.2004.07.029, 2004.

Zunckel, M., Koosailee, A., Yarwood, G., Maure, G., Venjonoka, K., van Tienhoven, A. M., and Otter, L.: Modelled surface ozone over southern Africa during the Cross Border Air Pollution Impact Assessment Project, Environmental Modelling & Software, 21, 911-924, doi:https://doi.org/10.1016/j.envsoft.2005.04.004, 2006.

Appendix A

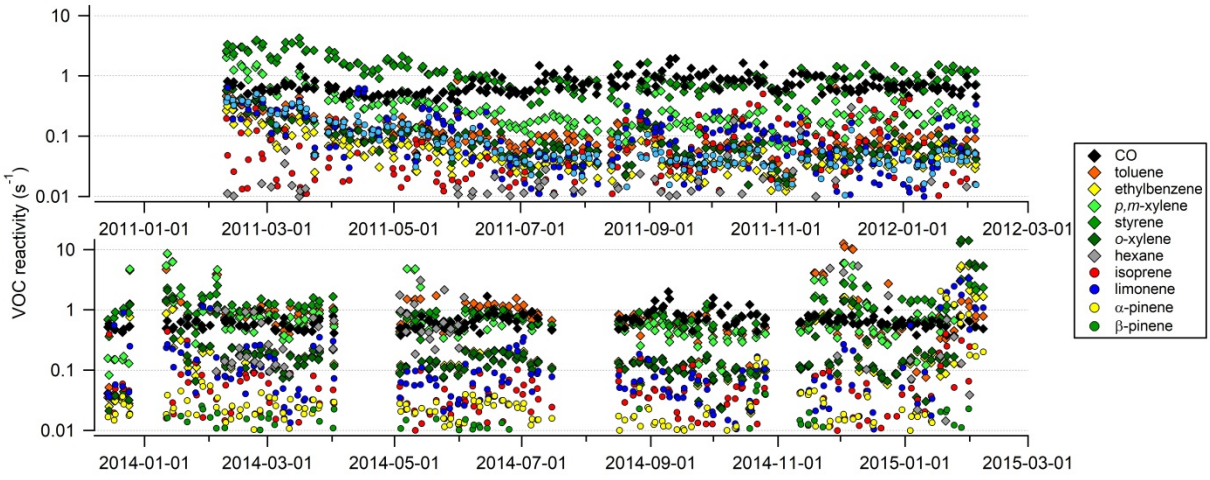

Fig. A1. Individual VOC reactivity time series. In the calculation of instantaneous O_3 production ($P(O_3)$), CO was treated as a VOC.

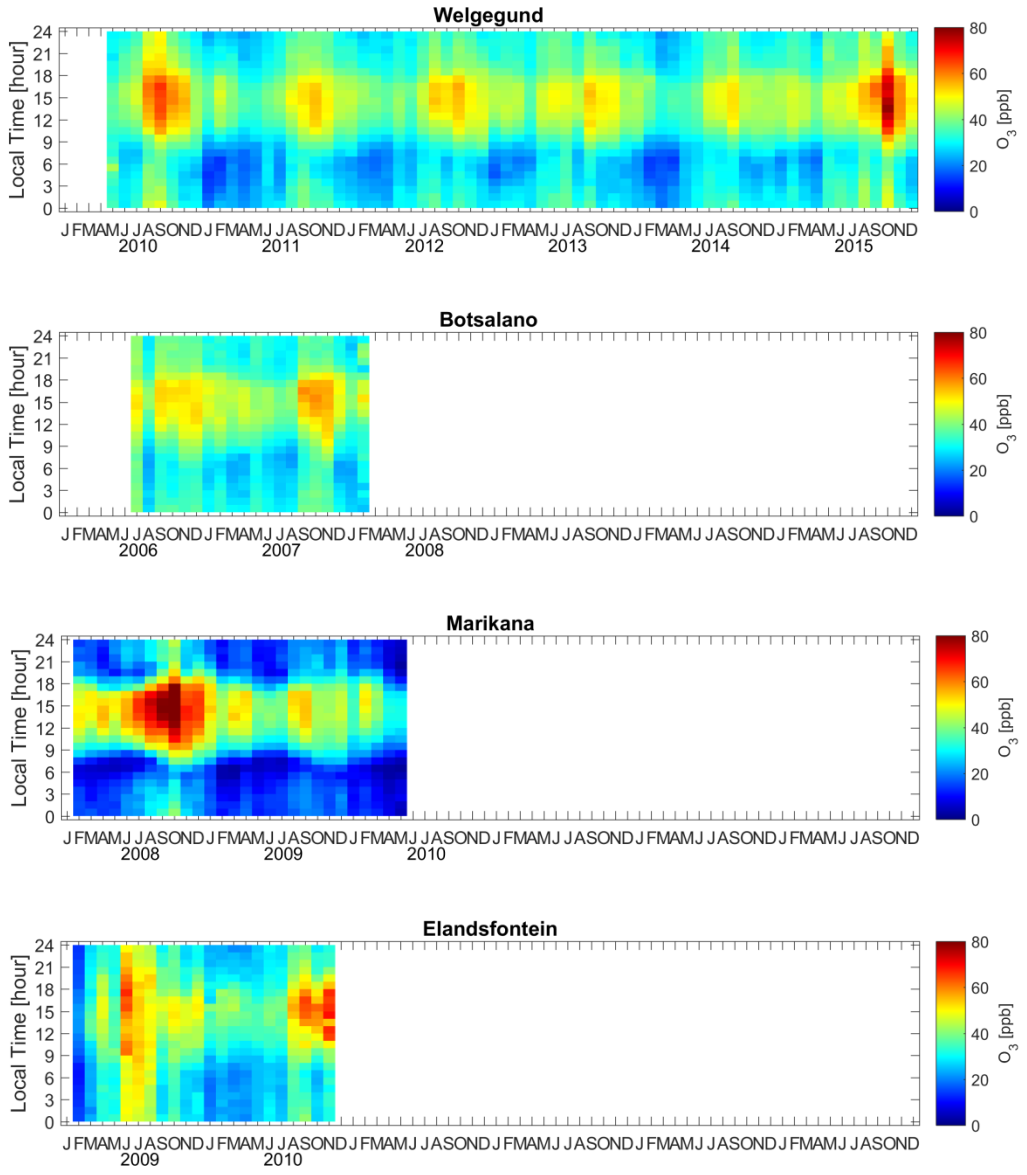

Fig. A2. Time series of monthly median O_3 concentrations for each hour of the day at the four sites

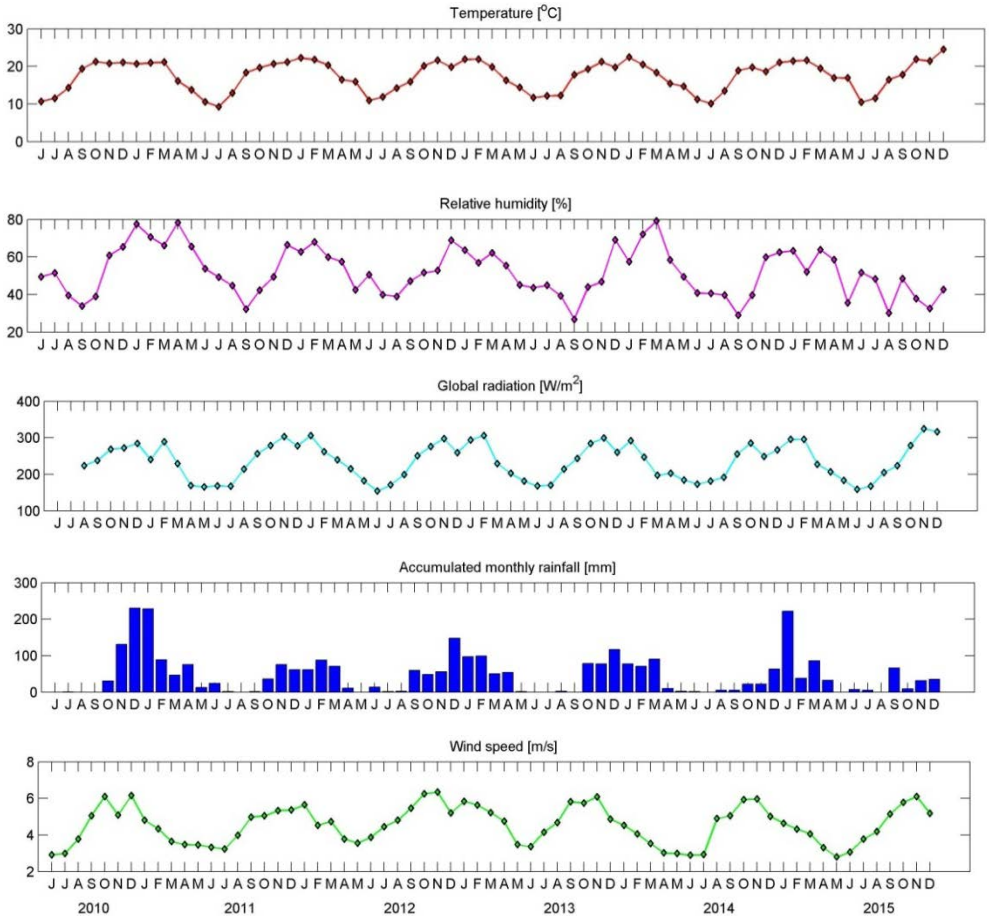

Fig. A3. Monthly averages of meteorological parameters at Welgegund to show typical seasonal patterns in continental South Africa. In the case of rainfall, the total monthly rainfall values are shown.

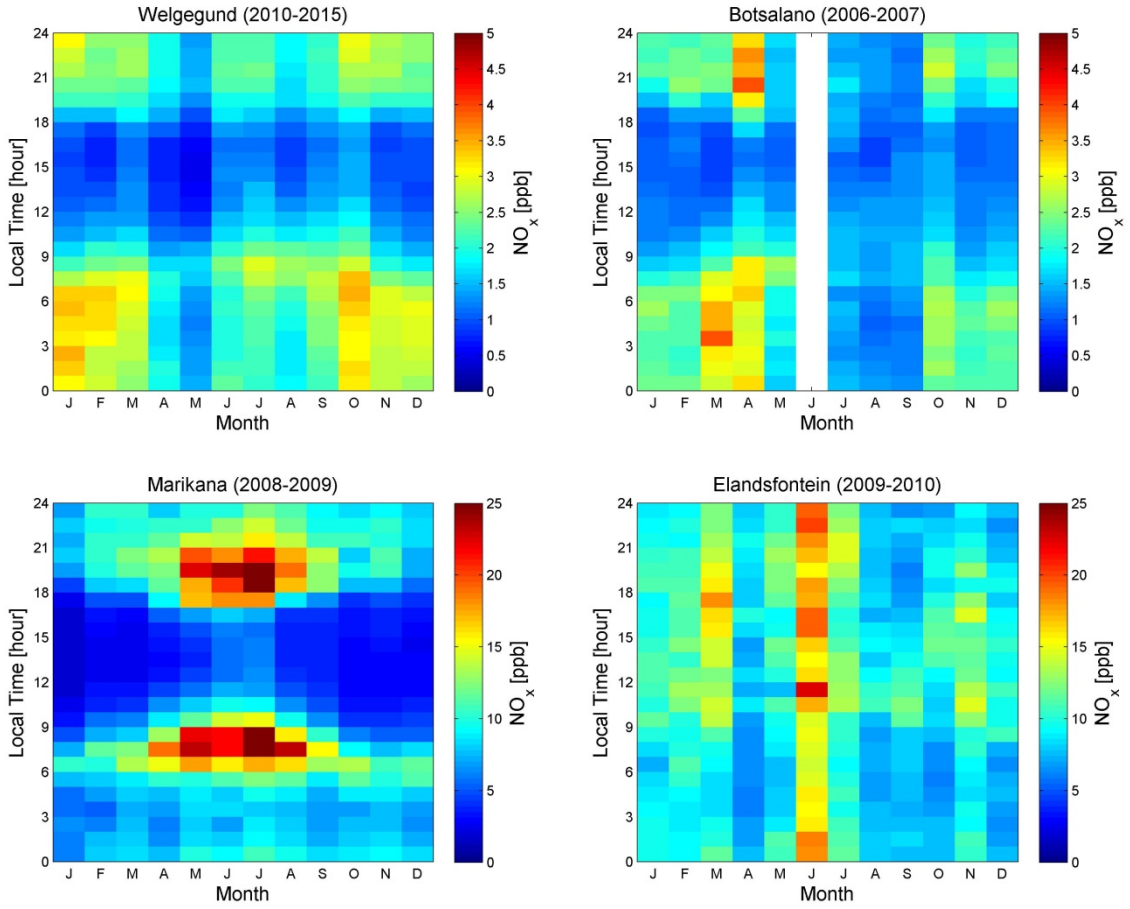

Fig. A4. Seasonal and diurnal variation of NO_x at Welgegund, Botsalano, Marikana and Elandsfontein (median values of NO_x concentration were used).

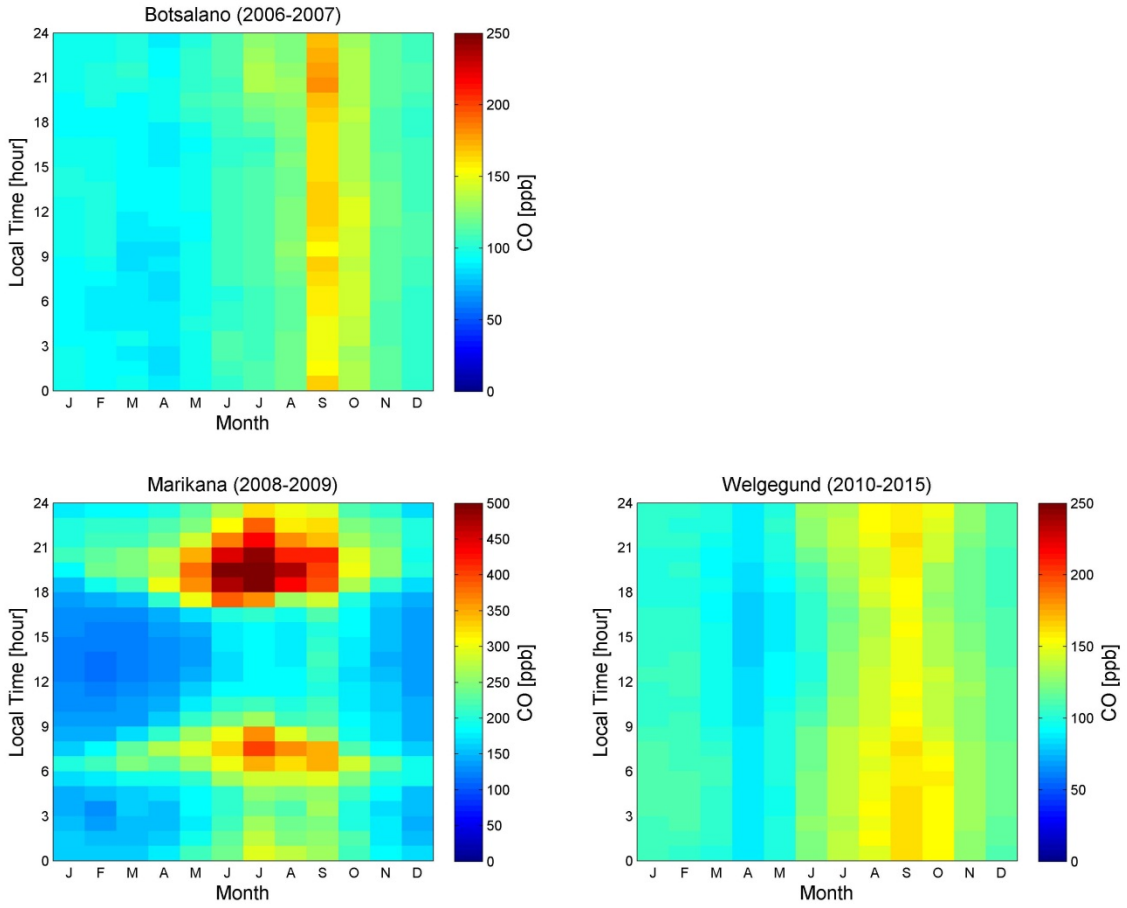

Fig. A5. Seasonal and diurnal variation of CO at Welgegund, Botsalano and Marikana (median values of CO concentration were used). Note that CO was not measured at Elandsfontein.

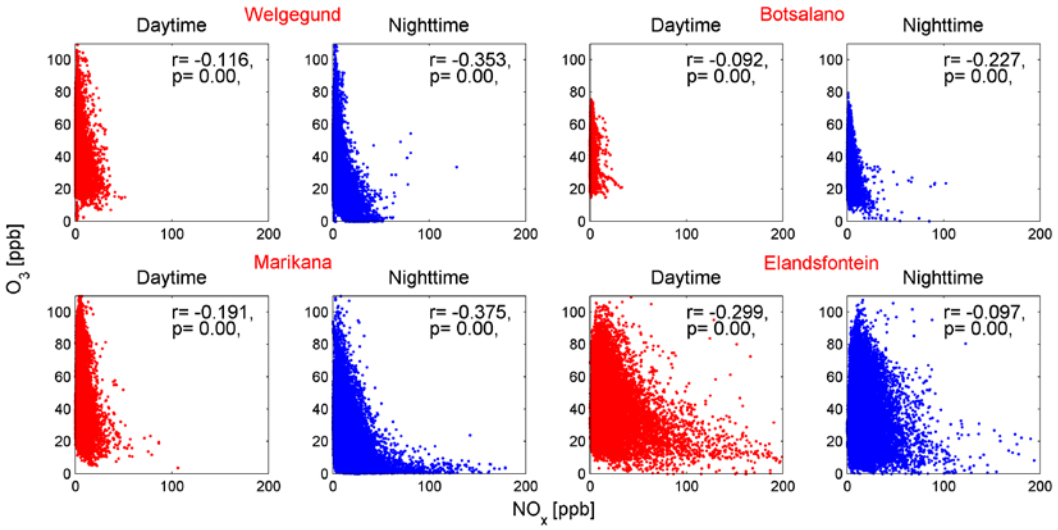

Fig. A6. Scatter plots of O_3 vs. NO_x for daytime (9:00 a.m. to 4:52 p.m.), and night-time (5:00 p.m. to 8:52 a.m.) at Welgegund, Botsalano and Marikana and Elandsfontein. The correlation coefficient (r) has a significance level of $p < 10^{-10}$, which means that r is statistically significant ($p < 0.01$).

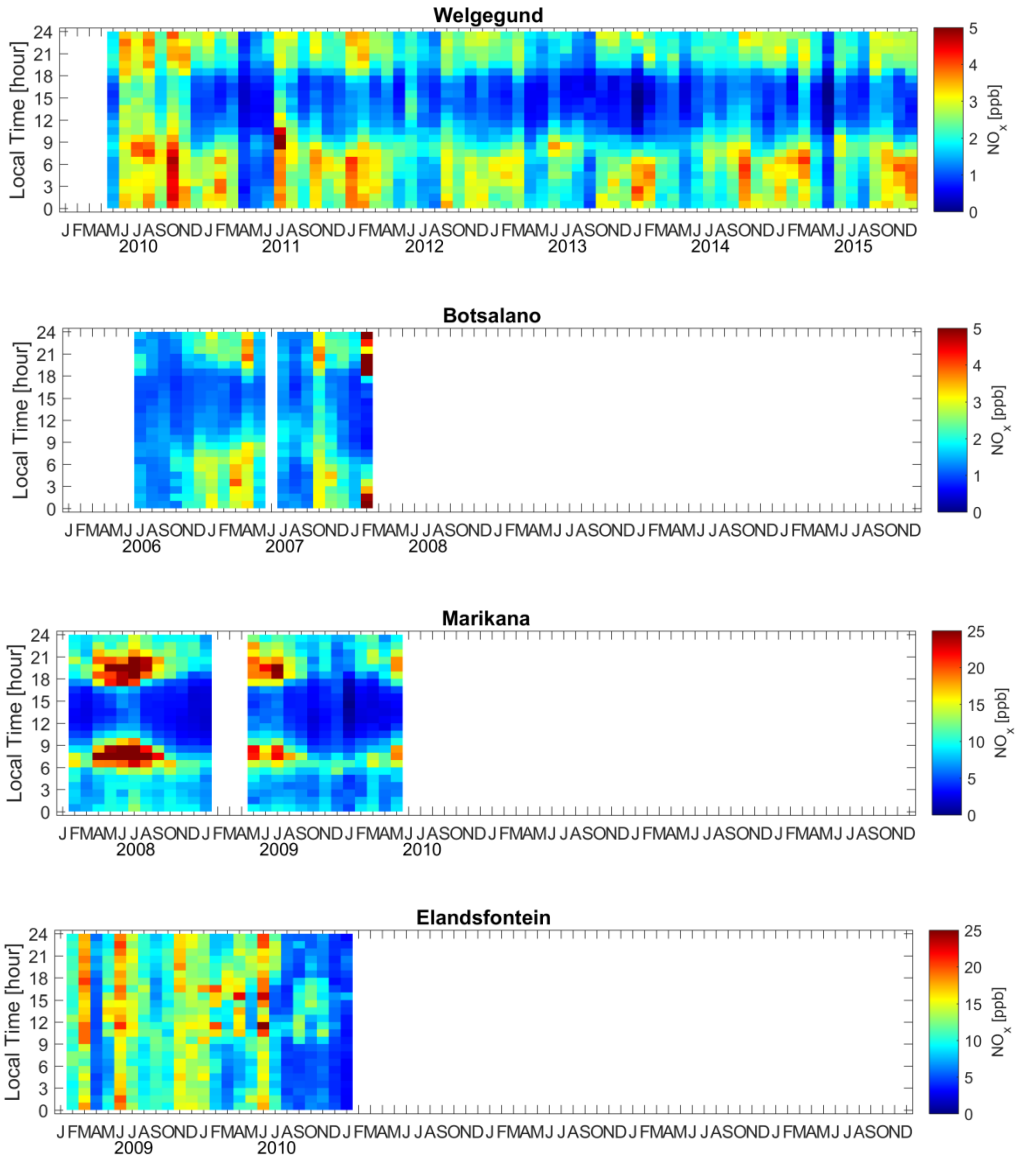

Fig. A7. Time series of monthly median NO_x concentrations for each hour of the day at the four sites

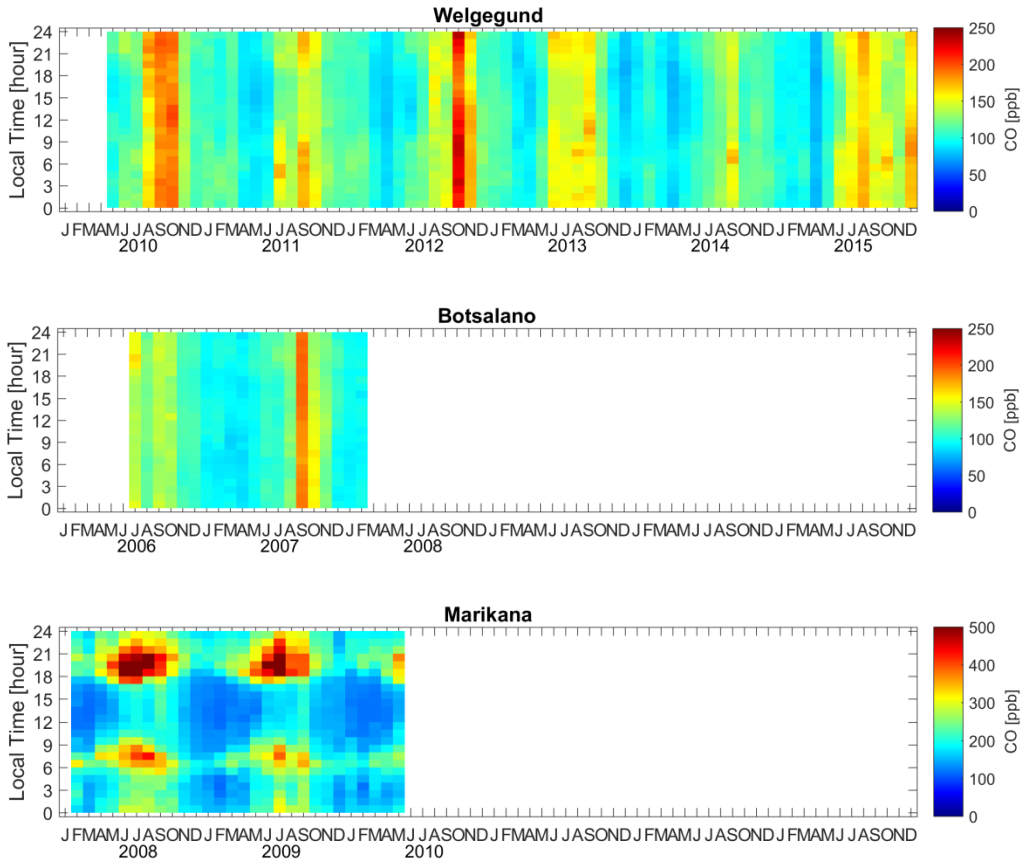

Fig. A8. Time series of monthly median CO concentrations for each hour of the day at the four sites